Fuel 327 (2022) 125148

Contents lists available at ScienceDirect

Fuel

journal homepage: www.elsevier.com/locate/fuel

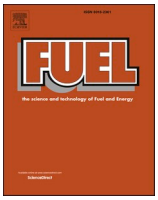

Kinetic modeling and reactor design of the direct synthesis of dimethyl ether for CO_2 valorization. A review

A. Ateka *, P. Rodriguez-Vega, J. Ereña, A.T. Aguayo, J. Bilbao

Department of Chemical Engineering, University of the Basque Country, UPV/EHU, P.O. Box 644, 48080 Bilbao, Spain

ARTICLE INFO

Keywords:
DME
CO_2 valorization
Fuels
Kinetic modeling
Deactivation
Membrane reactor

ABSTRACT

The direct synthesis of dimethyl ether (DME) is considered one of the most attractive routes for valorizing CO_2 and syngas on a large scale. DME has a high cetane number and its properties are similar to those of liquefied petroleum gases (LPG). It can be used directly as fuel, selectively converted into hydrocarbons (olefins, aromatics) or used as H_2 vector. This review explains briefly the advances in the study of the thermodynamics of DME synthesis and in the preparation of suitable catalysts. Subsequently, analyzes in detail the studies regarding the kinetic modeling, reactors design and reaction strategies. Extensive information is given on the kinetic models described in the literature, indicating the catalysts and reaction condition ranges for which the models were proposed. These kinetic models were whether based on those previously proposed separately for methanol synthesis and methanol dehydration stages on monofunctional catalysts, or models specifically proposed for bifunctional catalysts and conditions of the integrated process. Coke deposition is considered the main cause for catalyst deactivation and is quantified with different kinetic models. The presence of H_2O in the reaction medium is a limiting factor for the thermodynamics and for the extent of the reactions. This problem is overcome using hydrophilic membrane reactors, whose behavior has been studied by simulation and recently with an experimental system (with an LTA zeolite membrane). Finally, an analysis of the advantages and limitations of the different reactors and the challenges to progress towards the implementation of the direct CO_2 to DME synthesis process have been addressed.

1. Introduction

To respond to the challenge of reversing climate change, various agreements (Kyoto Protocol, Paris Agreement, Copenhagen Accord, Cancun Agreements, Climate Action Summit, among others) are focused on the mitigation of greenhouse gas emissions (GHG, primarily CO_2). The efficient use of energy, the circular economy, the rational symbiosis of the industrial development and the preservation of the natural environment are the main strategies to achieve the objective of net zero carbon emissions by 2050 [1,2]. Unfortunately, the setting up of these initiatives does not progress as the urgency and magnitude of the problem require. The causes that may hinder its implementation are mainly socioeconomic factors, such as the increased industrial activity in the developed countries, the difficulties transitioning away from the oil economy, the relocation of industries to developing countries, and the discovery of fossil fuel deposits, particularly of natural gas. This circumstance leads to estimate that in the next 20 years, fossil fuels will still be the main energy source all around the world [3]. Tao et al., [4] established a future scenario (Fig. 1) in which captured CO_2, together with biomass and wastes from the consumer society (plastics, tires), emerge as sustainable raw materials for manufacturing chemicals and fuels. The success of this change of raw materials requires developing new technologies, and intensifying the use of renewable energy sources, within the framework of the strategic sectors of Bio-Refinery [5,6], Waste-Refinery [7] and recycling (capture and use) of CO_2.

The limitations for the large-scale installation of the technologies for CO_2 capture and storage/sequestration (CCS) are their high cost and safety risks related to CO_2 leakage. There are currently 26 CCS projects in operation in the world (mainly in North America, Australia, China and Western Europe) and 21 in early stages of development [8]. Taking into account the environment in which the storage of CO_2 is carried out on a large scale, it can be done in [9–11]: i) Saline aquifers, ii) depleted oil and gas reservoirs, iii) coal beds, iv) deep ocean, and v) deep-sea sediments and minerals.

To finance the expensive investments required by CCS technologies, it is essential to promote CO_2 upgrading generating an economic benefit. Thus, the carbon capture, utilization and storage (CCUS) strategies

* Corresponding author.
E-mail address: ainara.ateka@ehu.eus (A. Ateka).

https://doi.org/10.1016/j.fuel.2022.125148
Received 23 February 2022; Received in revised form 14 June 2022; Accepted 29 June 2022

Nomenclature

a	Activity
C_i	Concentration of i compound
D	Gas effective dispersion coefficient, $m^2\ h^{-1}$
d	Sub index for deactivation
d_R	Reactor diameter, m
$D_{e,i}$	Effective diffusion coefficient of i compound, $m^2\ h^{-1}$
f_i	Fugacity of i compound, atm or bar
K_i	Adsorption equilibrium constant of i compound, atm^{-1} or bar^{-1}
K_N	Equilibrium constant of N reaction step
k_N	Kinetic constant of N reaction step
P, P_i	Total pressure and partial pressure of i compound, respectively, bar or atm
P_R, P_P	Total pressures at the reaction and permeation sections, respectively, atm
p	Vector of permeances of each i compound, mol $m^{-2}\ h^{-1}\ bar^{-1}$
r	Radial position in the catalyst particle
$\boldsymbol{r_c}$	Vector containing the reaction rates of each i compound and the deactivation rate
r_i	Formation rate of each i compound, typically $mol_C\ g^{-1}\ h^{-1}$
s_i	Source term, bar h^{-1}
T	Temperature, °C or K
$\mathbf{u_R}$, $\mathbf{u_P}$	Vectors of dependent variables on reaction and permeate sections, respectively, in packed bed membrane reactors
y_i	Molar fraction of i compound
z	Longitudinal position in the catalytic bed

Greek symbols

ΔP	Vector of pressure differences between the reaction and permeate sections for each i compound in packed bed membrane reactors, bar
β	Specific term defined for certain kinetic equations
ε	Effective porosity of the catalytic bed
θ_i, $\theta_{d,i}$	Term related to the attenuation of the reaction rate by i compound adsorption, and equivalent for deactivation
ν	Gas linear velocity, m h^{-1}

constitute the heart of a circular economy, integrating technologies of CO_2 capture and storage with CO_2 valorization technologies towards products of commercial interest, through net energy generation processes [12,13]. The utilization of non-fossil energy generation technologies (like solar energy) for H_2O electrolysis, allows the reduction of CO_2 net emission within the integrated processes [14].

The routes for upgrading CO_2 have received a great deal of attention in the literature, and different reviews have collected the fundamentals and advances of the different technologies, the modeling/simulation of the different processes and the energy and economic considerations that determine their installation [12–27]. Among these routes, the catalytic processes are of greater interest and have achieved remarkable technological development. In the following sections, these catalytic processes for valorizing CO_2 into fuels and chemicals are briefly described, highlighting the thermodynamic advantages of the direct synthesis of dimethyl ether (DME) and the interest of its applications as fuel and as raw material. Subsequently, this review analyzes in detail the main advances in two fundamental aspects for the implementation of the direct synthesis of DME from CO_2 hydrogenation, that is, the kinetic modeling and reactor design, where the hydrophilic membrane reactor currently draws attention.

2. Catalytic processes for CO_2 conversion

Due to the relevance of H_2 consumption in the economic viability of the CO_2 conversion process, Tao et al., [4] distinguished the processes for CO_2 transformation requiring H_2 as a reactant and those not requiring H_2.

2.1. Without H_2 as reactant

Some of these reactions (summarized in Fig. 2) are of great interest in the current energy transition period, but this interest will diminish when increasing the large-scale availability of H_2, generated by electrolysis of H_2O.

2.1.1. Oxidative coupling (OC)

This reaction is suitable for valorizing burgeoning natural gas reserves, in which CO_2 content may reach 10 % [28,29], and can be oriented towards the production of ethane (Eq. (1)) or ethylene, (Eq. (2)).

$$2CH_4 + CO_2 \rightarrow CH_3CH_3 + CO + H_2O \quad (1)$$

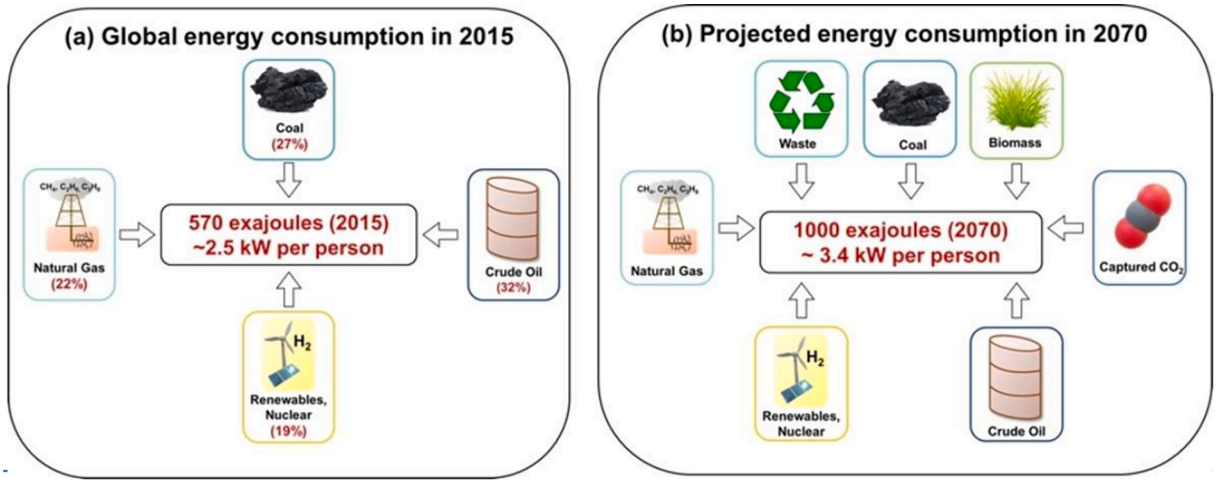

Fig. 1. Change in raw materials to meet foreseeable energy demand in 2070, without increasing GHG emissions. Reproduced from [4]

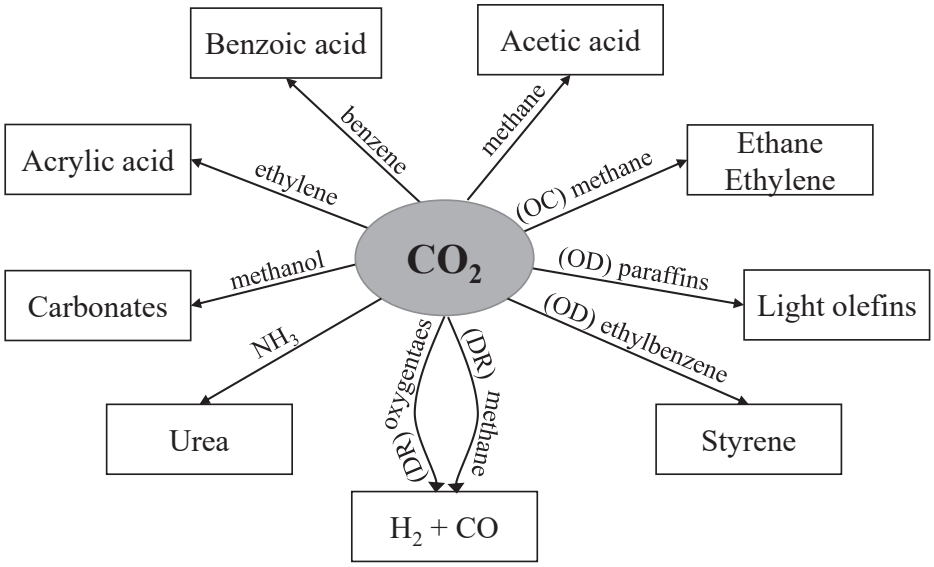

Fig. 2. Routes for CO_2 conversion without H_2 as reactant.

$$2CH_4 + 2CO_2 \rightarrow CH_2CH_2 + 2CO + 2H_2O \quad (2)$$

2.1.2. Oxidative dehydrogenation (OD)

The production of light olefins through oxidative dehydrogenation of their corresponding paraffins (ODP) (Eq. (3)), being ethane and propane the most studied, is an alternative to steam cracking, with lower energy requirement, and lower deactivation of the catalyst by coke [30,31].

$$C_nH_{n+2} + CO_2 \rightarrow C_nH_n + CO + H_2O \quad (3)$$

The oxidative dehydrogenation of ethylbenzene (ODE) to styrene (Eq. (4)) avoids the high steam requirement of the conventional industrial process without oxidant agent [32,33].

$$C_6H_5CH_2CH_3 + CO_2 \rightarrow C_6H_5CH = CH_2 + H_2O + CO \quad (4)$$

2.1.3. Dry reforming (DR)

The energy requirement is lower than in the steam reforming. It has been extensively studied for methane (MDR, Eq. (5)) [34–36] and has extended to the conversion of oxygenates derived from biomass (as ethanol (Eq. (6)), glycerol (Eq. (7)) and bio-oil).

$$CH_4 + CO_2 \rightarrow 2H_2 + 2CO \quad (5)$$

$$C_2H_5OH + CO_2 \rightarrow 3CO + 3H_2 \quad (6)$$

$$C_3H_8O_3 + CO_2 \rightarrow 4CO + 3H_2 + H_2O \quad (7)$$

These reactions have received less attention than bio-oxygenates steam reforming and the main challenge has been achieving catalyst stability [37,38].

2.1.4. Chemicals production

Among these reactions, the production of acetic acid (by the reaction of CO_2 with CH_4) and that of benzoic acid (with benzene) are relevant. Furthermore, acrylic acid production through the direct carboxylation of ethylene (Eq. (8)) is interesting to valorize the CO_2 generated in the ethylene production units by steam cracking of naphthas [39].

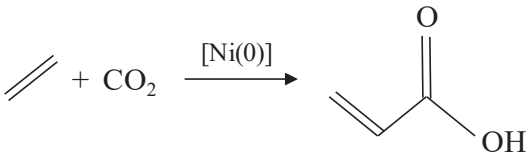

(8)

Dimethyl carbonate (DMC) $(CH_3O)_2CO$ is produced by reacting with methanol (Eq. (9)) [40].

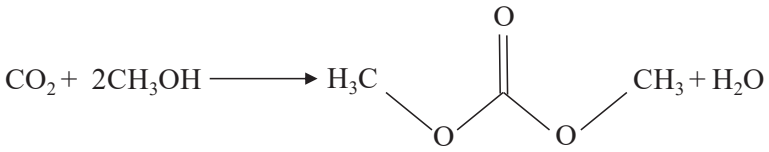

(9)

Cyclic carbonates (of ethylene, propylene, cyclohexane, styrene and others) are produced by the addition of CO_2 to an epoxy (Eq. (10)) [41].

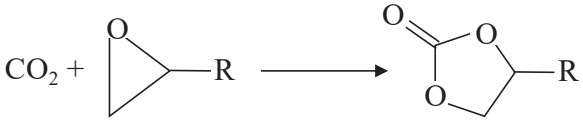

R = H for ethylene carbonate
R = CH_3 for propylene carbonate

(10)

Besides, CO_2 is valorized in the NH_3 production industry itself for the

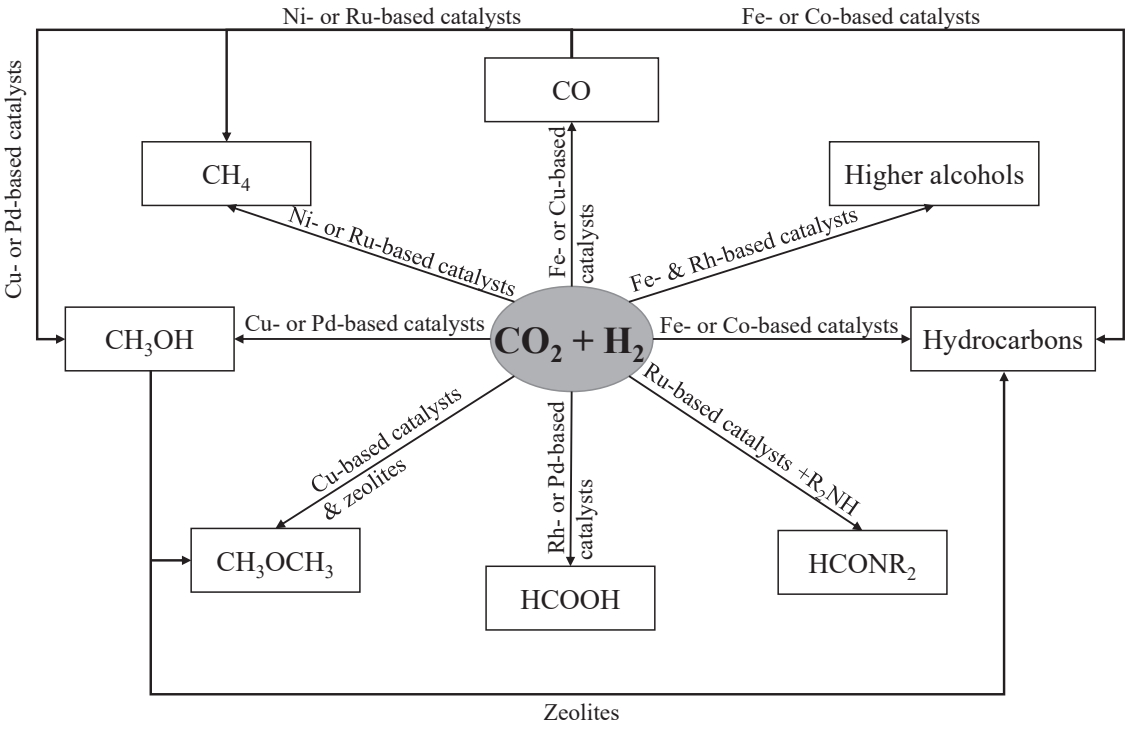

Fig. 3. Catalytic routes for CO_2 hydrogenation (adapted from the work by Vu et al., [47]. Copyright 2021, Elsevier).

synthesis of urea (carbamide, $(NH_2)_2CO$) in two stages, Eqs. (11) and (12) [42].

$$2NH_3 + CO_2 \rightleftharpoons H_2N - COONH_4 \quad (11)$$

$$H_2N - COONH_4 \rightleftharpoons (NH_2)_2CO + H_2O \quad (12)$$

2.2. CO_2 hydrogenation

The routes for the catalytic hydrogenation of CO_2, schematized in Fig. 3, are receiving increasing attention [43–49]. According to the target products the routes can be classified as: with C1 compounds as products (methane, carbon monoxide, methanol, formaldehyde); and those that form compounds with 2 or more carbon atoms (hydrocarbons and oxygenates). The state of technological development and industrial implementation is different, and conditioned by the different demand of the products on the market. Here below, a brief analysis of the main routes is conducted, and in Section 3, attention is focused on DME synthesis.

2.2.1. Methanation

CO_2 conversion and CH_4 selectivity in this reaction (Eq. (13)) are favored at high pressure and low temperature, and the results are good (almost complete conversion and selectivity close to 100 %) with the appropriate catalyst [50,51] according to the stoichiometry:

$$CO_2 + 4H_2 \rightleftharpoons CH_4 + 2H_2O \quad \Delta H^0_{298K} = -165.0kJ\ mol^{-1} \quad (13)$$

The improvement of the process using reactors with hydrophilic, steam-selective sodalite (SOD) membranes to replace conventional packed- or fluidized-bed reactors is relevant. The objectives are to reduce the thermodynamic limitations of the reaction and avoid catalyst deactivation by sintering [52,53].

2.2.2. Reverse water gas shift (rWGS)

The conversion of CO_2 by the rWGS reaction (Eq. (14)) is an endothermic reaction requiring high temperature (above 700 °C) to obtain considerable CO_2 conversion. The selection of the catalysts is conditioned by stability and selectivity requirements [54], and these associated with: i) The presence of oxygen vacancies; ii) the capability for adsorbing CO_2 and generating formate active species, and; iii) a weak binding energy of CO [55,56].

$$CO_2 + H_2 \rightleftharpoons CO + C_2O \quad \Delta H^0_{298K} = -41.2kJ\ mol^{-1} \quad (14)$$

2.2.3. Synthesis of Methanol

The thermodynamics of the exothermic synthesis of methanol from CO_2 (Eq. (15)) require low temperature and high pressure to attain remarkable conversion. However, given the low reactivity of CO_2, temperatures above 240 °C are required with conventional catalysts as to obtain notable reaction rate values. The challenges are oriented towards developing new, active, selective and stable catalysts [57–60], reactors and operating strategies [61]. The industrial reference, from the sustainability point of view, is the plant in Reykjavik (Iceland). Using geothermal energy, this plant has an annual capacity of 4,000 metric tons, valorizing 5,600 tons of CO_2 [62].

$$CO_2 + 3H_2 \rightleftharpoons CH_3OH + H_2O \quad \Delta H^0_{298K} = -49.5kJ\ mol^{-1} \quad (15)$$

2.2.4. Synthesis of Ethanol

This reaction (Eq. (16)) proceeds through a more complex mechanism than that for methanol synthesis [49] and requires selective multifunctional catalyst of complex composition [63].

$$2CO_2 + 6H_2 \rightleftharpoons C_2H_5OH + 3H_2O \quad \Delta H^0_{298K} = -86.7kJ\ mol^{-1} \quad (16)$$

2.2.5. Synthesis of hydrocarbons

In the direct production of hydrocarbons from CO_2 tandem catalysts are used in the same reactor, favoring the thermodynamic displacement and selectivity. The alternative routes comprise [45,64]: i) Modified Fischer-Tropsch synthesis (MFTS), incorporating a zeolite to the FT catalyst, and; ii) with methanol/DME as intermediates (Eq. (17)), combining a methanol/DME synthesis catalyst with a zeolite for their conversion into hydrocarbons [65]. The composition of the metal oxide

and in particular, its content of oxygen vacancies, is a key feature for the adsorption of CO_2 [58], while the selection of the shape selectivity and acidity of the zeolite allows the selective formation of light olefins, aromatics or isoparaffinic gasoline [66,67].

$$CO_2 + H_2 \Rightarrow CH_3OH/DME + H_2O \Rightarrow \begin{cases} Light\ olefins \\ Aromatics \\ Light\ paraffins \end{cases} \quad (17)$$

3. Dimethyl ether synthesis

The interest of DME synthesis stands out among the alternative routes for CO_2 valorization in Fig. 3, due to the applications of DME and the thermodynamic advantages for CO_2 conversion through the direct DME synthesis process.

3.1. Properties and economy of DME

DME (CH_3-O-CH_3) is a non-toxic oxygenate, with no impact on the environment, and with interesting properties for multiple applications [68–70]. It is widely used as aerosol, pesticide, ecological refrigerant, propellant (substituting chlorofluorocarbons), organic solvent [71] and as household fuel in Asian developing countries. Moreover, it has a great potential as automotive fuel since it can be easily adapted (similar to LPG) to compression ignition engines [72]; and gives way to lower greenhouse gas emissions than other fuels (CNG, LPG, Gasoline) [69]. The interest of DME as fuel for diesel engines is based on its properties. Its cetane number (CN), around 55, is higher than that of diesel (40–50) and its autoignition temperature (235 °C) and the air/fuel mass ratio (9) are lower (250 °C and 14.6, respectively for diesel). Consequently, it is usually used in mixture with LPG or diesel. A common mixture of 10–30% of DME in diesel has the advantage of reducing CO_2, soot and N and S oxide emissions [73].

The interest of DME as a raw material is growing, given its advantages over methanol in different fuels and raw materials (olefins and aromatics) production processes. Thus, DTO (dimethyl ether-to-olefins) process may replace or complement the MTO processes (methanol-to-olefins) of UOP Norsk Hydro [74] and MTP process (methanol-to-propylene) of Lurgi [75]. Among the advantages of the DTO process: i) It is performed at lower temperature because the DME is more reactive than methanol [76]; ii) HZSM-5 is suitable as catalyst, and its deactivation is slower than that of SAPO-34 in the conversion of methanol [77,78]. In addition, in the DTO process, the well-established technology for the MTO process can be used, with reactor-regenerator systems with catalyst circulation between units [79].

DME is also adequate as H_2 vector, through steam reforming using bifunctional catalysts [80]. Due to its characteristics, it can be used in proton exchange membrane fuel cells (PEMFC) [81] and solid oxide fuel cells (SOFC) [82], as well as for energy storage, through a cycle comprising DME synthesis from CO_2 (exothermic) and DME reforming to H_2 (endothermic), using energy intermittently generated from renewable sources [83].

3.2. Synthesis in two stages

The production of DME (10 Million tons/year, mostly in Asian countries) has been carried out using syngas feeds in a two-step process, that is, the synthesis of methanol and its dehydration towards DME [84]. The technology is currently revamping towards valorizing CO_2, with the encouragement that the cost of DME production is lower than that of alcohols (methanol, ethanol, butanol, octanol) and hydrocarbons (gasoline, diesel, kerosene) [85]. The conventional catalyst of the methanol synthesis unit is based on CuO-ZnO-Al_2O_3, and that of methanol dehydration in γ-Al_2O_3, of low manufacturing cost [86–88]. Catalysts with higher acidity and activity than γ-Al_2O_3 have also been studied, and the greatest research effort has focused on zeolites. HZSM-5 zeolite has received special attention, and its acidity has been modified as to minimize the presence of strong acidic sites [89,90]. Catizzone et al., [91,92] proposed ferrierite (FER) and reported higher reaction rates and lower coke deposition than with nano-sized HZSM-5 (MFI structure).

3.3. Direct synthesis

3.3.1. Thermodynamics

The reactions involved in the process comprise: methanol synthesis (Eqs. (15) and (18)), methanol dehydration (Eq. (19)), reverse water gas shift (rWGS) (Eq. (14)), and the secondary reaction of paraffins (mainly methane) formation (Eq. (20)).

$$CO + 3H_2 \rightleftharpoons CH_3OH + H_2O \quad (18)$$

$$2CH_3OH \rightleftharpoons CH_3OCH_3 + H_2O \quad (19)$$

$$nCO + (2n+1)H_2 \rightleftharpoons C_nH_{2n+2} + nH_2O \quad (n = 1-3) \quad (20)$$

The main interest of performing methanol dehydration (Eq. (19)) in the same reactor as methanol synthesis (Eqs. (15) and (18)) is the displacement of the thermodynamic equilibrium of these reactions, and as a consequence, easing the conversion of CO_2 [93]. Another consequence is that the process can be carried out at a higher temperature (higher reaction rate) and with a lower H_2/CO_x ratio than methanol synthesis, facilitating the joint valorization of CO_2 and syngas derived from biomass [94].

Ateka et al., [95] delved into the capacity of methanol synthesis (MS) and direct DME synthesis (DS) processes for the valorization of CO_2 and studied the effect of the reaction conditions (H_2 + CO + CO_2 mixture composition in the feed, temperature, pressure) on CO_2 conversion, MeOH and DME yield and selectivity, and on the heat generated. The study determined that effective CO_2 valorization was feasible both in MS and DS processes for CO_2/CO_x ratios in the feed over 0.5 within 250–300 °C range (Fig. 4). The study evidenced that the effect of the reaction conditions on DME yield differed from that on CO_2 conversion (opposite trends). Therefore, the optimal conditions corresponded to a compromise between the interest of DME production and CO_2 valorization.

3.3.2. Catalysts

The bifunctional catalysts for the direct synthesis of DME from CO_2

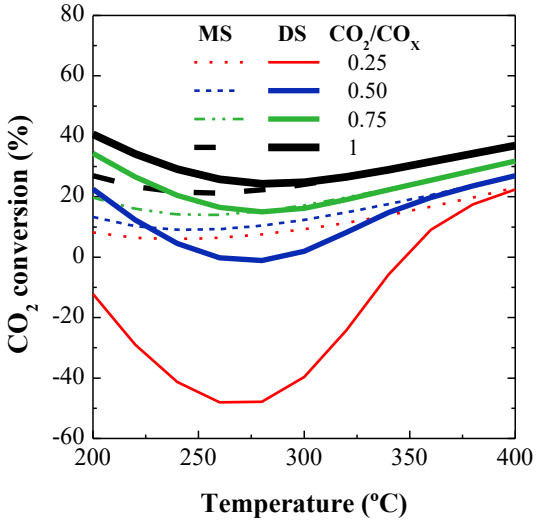

Fig. 4. Evolution of CO_2 conversion with temperature in the methanol synthesis (MS) and the direct DME synthesis (DS) processes for feeds of different CO_2 concentration. Adapted from the work by Ateka et al., [95]. Copyright 2017, Elsevier.

or CO_2 co-fed with syngas have been developed using as a basis the experience on catalysts for the stages of methanol synthesis and methanol dehydration to DME, and for the direct synthesis of DME from syngas ($H_2 + CO$), and taking into account the differences required in the reaction conditions and composition for this approach. These differences affect the composition and properties required for the activity, selectivity, stability and regenerability of the catalyst. Stability has received a great deal of attention because it is significantly relevant for the viability of the catalyst. Focusing on bi-functional catalysts for the direct synthesis of DME from syngas, Dadgar et al., [96] distinguished as main causes of deactivation: i) Coke deposition in the metallic catalyst, in the acid catalyst or in both; ii) sintering of the metallic catalyst, and iii) interactions between components of the metallic and acid catalysts. The challenge in the preparation of the catalyst is to minimize deactivation by avoiding irreversible deactivation (sintering or composition change), minimizing the effect of coke deposition (to prolong the lifetime prior to regeneration) and providing the catalyst the required hydrothermal stability for the complete recovery of its activity after regeneration by coke combustion.

In the direct synthesis of DME temperature is higher than in the synthesis of methanol, CO_2 conversion is favored, and the concentration of H_2O in the reaction medium is higher. This latter feature affects negatively the activity of the metallic function (usually based on CuO-ZnO-Al_2O_3), reducing the reaction rates of CO and CO_2 hydrogenation and of the WGS reaction [97–99], and favoring Cu oxidation and sintering [100]. The effect of H_2O on the activity of the acid dehydration catalyst (γ-Al_2O_3 and HZSM-5 are the most used) is complex. On the one hand, H_2O displaces the thermodynamic equilibrium and adsorbs competitively on the active sites diminishing their activity, but on the other hand, the presence of H_2O attenuates coke formation [101].

3.3.2.1. Catalysts for methanol synthesis. Multiple modifications of the CuO-ZnO-Al_2O_3 (CZA) catalysts, conventionally used for methanol synthesis, have been widely studied to favor the conversion of CO_2. ZnO has been replaced by La_2O_3, MgO, Fe_2O_3 and CeO_2 [102–105] as to promote CuO dispersion, catalyst stability and CO_x conversion. Al_2O_3 has also been replaced, partially or totally, by MnO [106], ZrO_2 [107–111], Ga_2O_3 [112,113] and TiO_2 [114]. And the favorable contribution of noble metals (Au, Pt, Pd, Rh) for promoting hydrogenation [115–121], and of the confinement in mesoporous matrixes [122] to boost the stability of Cu-ZnO catalysts has also been ascertained.

Moreover, Cu-based catalysts have been replaced by other alternatives, more active for CO_2 hydrogenation and without sintering problems. Among them, ZnO-ZrO_2 [123], In_2O_3, In_2O_3-ZrO_2 and In_2O_3-Ga [124–126] catalysts and those based on Co [127] or on novel metals with different supports and promoters [128,129]. A relevant challenge in the catalysts used for CO_2 conversion is to minimize the extent of CO formation by means of the rWGS reaction. For this purpose, among the transition metal catalysts, those containing Co [130] are interesting. Among those composed with noble metals Pd-Zn [131,132] and also In_2O_3 have a selective performance [133].

3.3.2.2. Catalysts for methanol dehydration. Due to its low cost and high selectivity, γ-Al_2O_3 has been commonly used [87,134], although the studies are oriented to the use of other less hydrophilic acid catalysts of limited acid strength, as to avoid the formation of hydrocarbons [135]. Framework types as BEA, EUO, FER, MOR, MTW, TON [136,137] and more frequently MFI type (HZSM-5) [138,139] and silicoaluminophosphates (SAPO-11, −18, −34) are used [140]. Indeed, a great deal of effort has been placed on tailoring HZSM-5 catalysts, pursuing hydrothermal stability and deactivation resistance [140–142]. SAPO-11 [108,143] and ferrierite [136,144,145] catalysts are also suitable for these purposes.

3.3.2.3. Configuration of the bifunctional catalyst. The configuration of the bifunctional catalyst has received a great deal of attention as to promote the synergy advantages of the tandem catalysts while avoiding their problems [146]. The arrangement in a single hybrid catalyst particle favors the rapid dehydration of methanol in sites adjacent to those where it was formed [147], although the blockage of the inlet of the zeolite pores by the metallic function in the extrusion/pelletizing stage must be avoided [148]. Besides, an intimate contact between both functions may lead to ionic transport phenomena (of Cu^+ and Al^{3+}) contributing to deactivation [149].

The core–shell structure (depositing one function over a nucleus of the other) has been explored as an alternative to hybrid catalysts [150,151]. Sánchez-Contador et al., [152,153] tested a CuO-ZnO-ZrO_2@SAPO-11 core–shell catalyst and ascertained that this configuration prevented the partial blockage of SAPO-11 mesopores by CuO-ZnO-ZrO_2 particles in the pelletizing step used for preparing hybrid catalysts. Feeding $H_2 + CO_2 + CO$ mixtures in a CO_2/CO_x ratio of 0.5, a DME yield ~ 9 % per pass and selectivity over 80 % were achieved with this core–shell catalyst, whereas 7 % and 77 %, respectively, for the hybrid system composed of the same metallic and acid function at 325 °C, 30 bar and 7.6 g_{cat} h mol_C^{-1}.

3.3.3. Reactors for syngas conversion

The synthesis of DME has been studied with different reactors of conventional configuration and successively innovations have been carried out to improve the yield and selectivity of DME and the energy efficiency of the process [70,154].

3.3.3.1. Conventional configuration. The interest of slurry phase (stirred or bubbling) reactors in the direct synthesis of DME and in other exothermic gas–liquid-solid reactions lies in their simple construction and temperature control, avoiding hot spots generation, due to the efficient heat transfer in the slurry with the heat exchanger tubes. Various authors have used this technology for the direct synthesis of DME from syngas in studies aimed at preparing suitable catalysts [155], kinetic modeling [156], design of the reactor and catalyst recirculation system [157,158] and optimizing operating conditions [159–161]. However, the slurry reactor presents mass transfer limitations and difficulties for the catalyst, which requires wettability conditions, mechanical resistance and non-aggregatibility [162]. Aoki et al., [163] provided the operating conditions of a pilot plant with a capacity of 100 tons per day of DME from syngas.

In the packed bed reactor, the heat transfer between phases is favored by the relative velocity of the flow with respect to the catalyst. The facility to operate in adiabatic regime or with heat transmission are other advantages. These allow for establishing a decreasing temperature profile, suitable for exothermic reactions as has been optimized for the conversion of methanol to DME [164]. However, the packed bed reactor requires precise control of the reaction conditions to avoid the formation of hot spots and the consequent sintering of the catalyst. Thus, the conversion is reduced to avoid excessive heat generation, requiring high syngas recycling. The heat transfer capacity increases using multitubular reactor systems (parallel packed beds) as simulated by Peláez et al., [165]. Song et al., [166] established a one-dimensional model to simulate a pilot-scale plant of DME synthesis, with shell and packed bed reactors, with capacity of 25–28 $Nm^3\ h^{-1}$ of syngas, determined the effect of the operation variables and validated the results experimentally.

The use of the fluidized bed reactors has also been studied by means of simulation and experimentally [167]. In this reactor, temperature is uniform due to the catalyst mixing regime, avoiding the formation of hot spots. In addition, the rate of heat transfer between phases is high. Abashar et al., [168] studied the potential capacity to increase the performance and selectivity of a dual-bed reactor with two fluidized beds in series. Koyunoğlu et al., [169] determined by Computation Fluid

Dynamics (CFD) a bed density of 2200 kg m^{-3} for maximum solid–gas contact. The limitations of the fluidized bed reactor are the need for a catalyst with high mechanical resistance to avoid mass losses due to attrition, and the demanding control of fluid dynamics to avoid any flow by-pass.

3.3.3.2. Innovative reactors. The advances in the design of the reactor for the direct synthesis of DME seek to increase energy efficiency and simplify the process, by integrating the reaction, heat exchange and separation stages. In the innovations studied through simulation (mainly from syngas as reactant) the following can be distinguished [70,154]: Coupled and dual type reactors, catalytic distillation reactors, membrane reactors, spherical reactors, microreactors and microchanell reactors.

Yousefi et al., [170] relied on the heat exchange capacity of the multitubular reactors, to reduce the thermodynamic barrier of DME synthesis from syngas in a dual reactor system, consisting of fluidized bed reactors. The strategy consisted of disposing the catalyst in the vertical tubes of the first reactor (water-cooled) and in the shell side of the second, where the reactions take place, producing methanol. To this second reactor syngas was fed together with the output stream of the first reactor, where it was preheated by flowing in counter-current with reacting gas mixture in the shell side. Thus, an autothermal regime was generated in the system, and in the second reactor a decreasing temperature profile with the reactor length, which favored the conversion of syngas and methanol into DME. Vakili et al., [171] designed a thermally coupled multitubular heat exchanger reactor, performing an endothermic reaction (cyclohexane dehydrogenation) in the shell side and the synthesis of DME in the inside tubes, with packed beds on both sides. Catalytic distillation is another process intensification strategy that has been studied for methanol dehydration, proving that intensifies DME production, reduces the energy requirement and avoids the costs of the separation unit [172,173].

Farsi et al., [174] studied a dual membrane reactor for DME production from syngas. The reaction system had three concentric tubes, being the catalytic bed placed in the intermediate tube. Water circulated to the inner tube's sweeping zone through a permselective membrane, and H_2 circulated from the outer sweeping zone to the reaction zone through a hydrogen permselective membrane. The external tube was surrounded by boiling water in order to remove the generated heat. The interest of feeding H_2 through a permselective Pd-based membrane was analyzed by Mardanpour et al., [175]. Farniaei et al., [176] integrated the two membranes with the dual reactor in the same reaction unit, using the heat generated in the synthesis of DME to provide the energy required for the dehydrogenation of cyclohexane. Bakhtyari et al., [177] integrated methyl formate production as endothermic reaction in the dual membrane reactor together with DME synthesis. Yasari et al., [178] addressed theoretically the unfavorable effect of H_2O separation on intensifying catalyst deactivation by coke and paraffin formation (trade-off); together with the favorable effect of increasing DME yield. This proves the advantages of a multi- stage double shell-and-tube reactor compared to the conventional single-stage packed bed reactor due to the improved heat removal and H_2O removing capacity. Bayat and Asil [179] designed a multifunctional moving bed reactor in which H_2O was adsorbed *in situ* with a regenerative 4A zeolite fed together with syngas, calculating a 31% increase in DME yield compared to a conventional packed bed reactor. The use of adsorption and of hydrophilic membrane strategies for the separation of water from the reaction medium takes a relevant importance when increasing the concentration of CO_2 in the feed, and therefore, greater attention is paid to this strategy in section 5.3.

The use of spherical reactors has advantages over tubular packed beds, such as lower pressure drop and smaller catalyst particle size (minimizing diffusion limitations). Samimi et al., [180], established a simulation model for the conversion of methanol to DME in a spherical membrane reactor. Subsequently, these same authors studied the conversion of methanol into DME in a system of two spherical reactors of axial flow arranged in series [181]. Farsi et al., [182] optimized the conditions for the production of DME from methanol in a multi-stage spherical reactor with axial flow and compared the performance of this configuration with the conventional tubular reactor. Farsi [183] quantified the advantages integrating hydrophilic membranes in each stage of a multi-stage radial flow spherical reactors for the production of DME from methanol, due to the shift of the thermodynamic equilibrium limitation.

Microchannel reactors are suitable for exothermic reactions that require good temperature control and contact between phases. Their high contact surface area to volume ratio facilitates mass and heat transfer and increases productivity. Hu et al., [184] studied experimentally the effect of the reaction conditions (temperature, pressure, residence time) on the direct synthesis of DME from syngas using a microchannel reactor. The higher yield, compared to a conventional packed bed reactor, was attributed to the shortening of bulk diffusion length, minimizing back mixing and increased accessibility of the gas to the catalyst surface. Hayer et al., [185] established and experimentally validated a 2D pseudo-homogeneous simulation model of these microchannel reactors in the direct synthesis of DME from syngas. The same authors [186] studied the effect of the fluid dynamics of different micropacked bed reactor-heat exchanger configurations on their performance. The high DME yields attained evidence the potential of these reactors and their ability to be improved by optimizing their fluid dynamics, which also depends on the reaction conditions. Pérez Miqueo et al., [187] compared the performance of different structured analytic reactors, verifying that the mass and heat transfer is independent of the substrates nature and shape (parallel cell, monoliths and open foams) and that these reactors allow working in isothermal regime with a volumetric productivity up to 0.20 (L of DME) h^{-1} cm^{-3} at 573 K.

4. Kinetic modeling

The first kinetic models established for the direct synthesis of DME combined the models proposed in the literature for the stages of methanol synthesis (mainly from syngas) and methanol dehydration to DME [156,167,188,189]. For methanol synthesis, Natta [190] proposed a pioneering model for ZnO/CrO_3 catalysts, and the model proposed by Leonov et al., [191] is considered the first for Cu based catalysts ($CuO-ZnO-Al_2O_3$). These models have continuously been improved, either considering the contribution of CO_2 conversion [192–194] and of the WGS reaction [195–197]; and various comparisons among the different available models have also been reported [198]. Likewise, different kinetic models have been proposed for methanol dehydration, based either on the Langmuir-Hinshelwood [199] or Eley-Rideal [200] postulates, or of empirical nature. For instance, those considering the inhibiting effect of H_2O in the reaction medium on the reaction rate expressions [201]. These models have been gathered and compared mainly for γ-Al_2O_3 and HZSM-5 based catalysts [202,203].

Nonetheless, the direct DME synthesis process is conducted under different conditions to those settled as optimal for each individual step. Indeed, the direct synthesis process is performed at higher temperature than methanol synthesis and higher pressure than that required for its dehydration. Bearing these in mind, specific models for the direct process have been developed [204,205]. Besides, deactivation has been considered [100,206], and modifications have been introduced for accurately describing the performance of catalysts with different configurations [97–99,207]. The kinetic models are described below, distinguishing those based on models proposed in the literature for individual stages (Section 4.1) from those specifically proposed for the direct process using new kinetic expressions (Section 4.2). In Table 1 the operating conditions for the application and main considerations of these models are summarized. For an overall view, the kinetic parameters along with the reactions considered in each scheme are gathered in

Table A.1 in the Supporting Information.

4.1. Based on combining models proposed for the individual reaction stages

The pioneering model of Ng et al., [188] for the direct synthesis of DME in a dual bed of commercial CuO-ZnO-Al_2O_3 and γ-Al_2O_3 catalysts was a combination of the: i) Kinetic model proposed by Vanden Bussche and Froment [194] for methanol synthesis (Eq. (21)), established considering the sequential reaction of CO to CO_2 to methanol (MeOH) through surface carbonates; with ii) that proposed by Berčič and Levec [208] for methanol dehydration (Eq. (22)) proceeding through dissociative adsorption. In the model, the kinetics of the rWGS reaction (Eq. (23)), was considered but not the methanation reaction (Eq. (13)) nor catalyst deactivation. The accuracy of the model was tested for fitting the experimental results obtained in a gradientless internal-recycle continuous reactor at 250 °C and 5 MPa for a variety of feedstock compositions (various CO_2 concentrations and H_2/CO_x ratios in the feed) and catalyst loadings. Except for high space velocities and large acid catalyst/metallic catalyst ratios, the model simulated quite satisfactorily. Ng et al., [188] reported for the first time the strong synergy obtained in the direct process, specially with CO rich feeds, due to the effective removal of methanol by dehydration and the product H_2O by the WGS reaction; whereas the extent of the synergy declined with increasing CO_2 concentration in the feed, since the reverse water–gas-shift reaction was favored leading to large amounts of H_2O.

$$r_{CO_2\ to\ MeOH} = \left[\frac{k_1 (P_{H_2} P_{CO_2}) \left(1 - \frac{P_{MeOH} P_{H_2O}}{K_{eqm1} \left(P_{CO_2} P_{H_2}^3 \right)} \right)}{\left(1 + K_2 (P_{H_2O}/P_{H_2}) + \sqrt{K_3 P_{H_2}} + K_4 P_{H_2O} \right)^3} \right] \tag{21}$$

$$r_{MeOH\ dehydration} = \left[\frac{k_6 K_{CH_3OH}^3 \left[C_{MeOH}^2 - \left(\frac{C_{H_2O} C_{DME}}{K_{eqm3}} \right) \right]}{\left(1 + 2\sqrt{K_{MeOH} C_{MeOH}} + K_{H_2O} C_{H_2O} \right)^4} \right] \tag{22}$$

$$r_{rWGS} = \left[\frac{k_5 p_{CO_2} \left(1 - \frac{P_{CO} P_{H_2O}}{K_{eqm2} \left(P_{CO_2} PH_2 \right)} \right)}{\left(1 + K_2 (P_{H_2O}/P_{H_2}) + \sqrt{K_3 P_{H_2}} + K_4 P_{H_2O} \right)} \right] \tag{23}$$

The kinetic parameters and equilibrium constants were defined according to Eq. (24), and the values for A(i) and B(i) are listed in Table A.1.

$$k_i = A(i) exp \left[\frac{B(i)}{RT} \right] \tag{24}$$

Lu et al., [167] addressed the kinetic modeling of the hybrid Cu-ZnO-Al_2O_3/HZSM-5 catalysts performance on laboratory scale fluidized bed reactor for CO hydrogenation. The model (Table A.1) considered methanol formation through CO_2 (Eq. (25)), methanol dehydration (Eq. (26)) and WGS reaction (Eq. (27)), and used the (CO_2, H_2, CO) adsorption constants established by Vanden Bussche and Froment [194] but neglected those for methanol and water, based on the low amount registered in the product stream in the experimental data. The model demonstrated to fit the experimental data obtained within the following conditions: 250–270 °C, 20–40 bar, H_2/CO ratio between 0.75 and 2, for SV of 3000 mL $g_{cat}^{-1} h^{-1}$.

$$r_{CO_2\ to\ MeOH} = \left[\frac{K_1 (P_{CO_2} P_{H_2}) \left(1 - \frac{P_{H_2O} P_{MeOH}}{K_{P,1} \left(P_{CO_2} P_{H_2}^3 \right)} \right)}{\left(1 + K_{CO_2} P_{CO_2} + K_{CO} P_{CO} + \sqrt{K_{H_2} P_{H_2}} \right)^3} \right] \tag{25}$$

$$r_{MeOH\ dehydration} = K_2 \left(\frac{P_{MeOH}^2}{P_{H_2O}} - \frac{P_{DME}}{K_{P,2}} \right) \tag{26}$$

$$r_{WGS} = \left[\frac{K_3 \left(P_{H_2O} - \frac{P_{CO_2} P_{H_2}}{K_{P,3} P_{CO}} \right)}{\left(1 + K_{CO_2} P_{CO_2} + K_{CO} P_{CO} + \sqrt{K_{H_2} P_{H_2}} \right)} \right] \tag{27}$$

Nie et al., [209] presented a Langmuir-Hinshelwood (LHHW) mechanism based model (Table A.1) from the results obtained in a packed bed integral reactor at 220–260 °C and 30–70 bar, for a bifunctional catalyst composed of commercial methanol synthesis and dehydration catalysts. The reaction rates considered in the model correspond to: methanol formation from CO (Eq. (28)) and from CO_2 (Eq. (29)) separately, methanol dehydration (Eq. (30)) and that for the WGS reaction (Eq. (31)). For the calculation of the kinetic parameters best fitting the experimental results the simplex method and genetic algorithm were combined. The model resulted reliable for describing the performance of the catalyst even for N_2 containing syngas feeds. Shim et al., [205] applied the model proposed by Nie et al., [209] and recalculated the kinetic parameters to best fit their experimental results obtained at industrial operating conditions.

$$r_{CO\ to\ MeOH} = \left[\frac{k_1 f_{CO} f_{H_2}^2 (1 - \beta_1)}{\left(1 + K_{CO} f_{CO} + K_{CO_2} f_{CO_2} + K_{H_2} f_{H_2} \right)^3} \right] \quad \text{being: } \beta_1 = \frac{f_{MeOH}}{K_{f_1} f_{CO} f_{H_2}^2} \tag{28}$$

$$r_{CO_2\ to\ MeOH} = \left[\frac{k_2 f_{CO_2} f_{H_2}^3 (1 - \beta_2)}{\left(1 + K_{CO} f_{CO} + K_{CO_2} f_{CO_2} + K_{H_2} f_{H_2} \right)^4} \right] \quad \text{being: } \beta_2 = \frac{f_{MeOH} f_{H_2O}}{K_{f_2} f_{CO_2} f_{H_2}^3} \tag{29}$$

$$r_{MeOH\ dehydration} = \left[\frac{k_3 f_{MeOH} (1 - \beta_3)}{\left(1 + \sqrt{K_{MeOH} f_{MeOH}} \right)^2} \right] \quad \text{being: } \beta_3 = \frac{f_{DME} f_{H_2O}}{K_{f_3} f_{MeOH}^2} \tag{30}$$

$$r_{WGS} = \left[\frac{k_4 f_{H_2O} (1 - \beta_4)}{1 + K_{CO} f_{CO} + K_{CO_2} f_{CO_2} + \sqrt{K_{H_2} f_{H_2}}} \right] \tag{31}$$

Hadipour et al., [189] (Table A.1) combined and recalculated the models proposed by Graaf et al., [196,197] for the transformation of syngas into methanol and that proposed by Berčič and Levec [208] for describing the rate of methanol dehydration to DME over a conventional CuO-ZnO-Al_2O_3/γ-Al_2O_3 hybrid catalyst. In both stages LH mechanisms were therefore assumed. In the methanol synthesis reaction rate (Eq. (32)), hydrogen was supposed to be dissociatively adsorbed in certain active sites competing with H_2O, whereas CO on different type of active sites competing with CO_2. On the other hand, in the dehydration stage (Eq. (33)), a LH surface controlled reaction with dissociative adsorption of methanol was found to best represent the experimental results. In the latter stage, DME adsorption term was neglected and the term

considering methanol partial pressure considered the driving force term. The model was capable for describing the experimental results in an agreement degree of 90–95 % for 230–300 °C range, 8 bar and space time values between 206 and 2240 g $mol^{-1}min^{-1}$.

$$r_{CO\ to\ MeOH} = \left[\frac{k_1 \left(P_{CO} P_{H_2}^{1/2} - \frac{P_{MeOH}}{KP1 \left(p_{CO_2} P_{H_2}^{1/2} \right)} \right)}{(1 + k_2 P_{CO} + k_3 P_{CO_2}) \left(P_{H_2}^{1/2} + k_4 P_{H_2O} \right)} \right] \quad (32)$$

$$r_{MeOH\ dehydration} = \left[\frac{k_5 \left(P_{MeOH}^2 - \frac{P_{H_2O} P_{DME}}{KP2} \right)}{\left(1 + 2(k_6 P_{MeOH})^{1/2} + k_7 P_{H_2O} \right)^4} \right] \quad (33)$$

Likewise, Moradi et al., [156] (Table A.1) considered the kinetics proposed by Graaf et al., [196,197] and Berčič and Levec [208], in this case for studying the intrinsic kinetics for DME synthesis from syngas in liquid phase (LPDME) over CuO-ZnO-Al_2O_3/HZSM-5 hybrid catalysts. Neglecting mass transfer resistance, gas- and liquid-phases were assumed to be in thermodynamic equilibrium and so, the kinetic rate expressions were based on components fugacity. Here the reactions of CO hydrogenation to methanol (Eq. (34)), WGS and methanol dehydration to DME (Eq. (35)) were considered, and the reparameterizing of the kinetic coefficients (following Arrhenius and Vanít Hoff equations) permitted obtaining apparent activation energies, reported to be 115 kJ mol^{-1} and 82 kJ mol^{-1} for methanol synthesis and dehydration, respectively.

$$r_{CO\ to\ MeOH} = \left[\frac{k_1 K_{CO} \left(f_{CO} f_{H_2}^{3/2} - \frac{f_{MeOH}}{f_{H_2}^{1/2} K_{fCO}} \right)}{\left(1 + K_{CO} f_{CO} + K_{CO_2} f_{CO_2} \right) \left(f_{H_2}^{1/2} + \frac{K_{H_2O} f_{H_2O}}{K_{H_2}^{1/2}} \right)} \right] \quad (34)$$

$$r_{MeOH\ dehydration} = \left[\frac{k_2 K_{MeOH}^2 \left(C_{MeOH}^2 - \frac{C_{H_2O} C_{DME}}{K_{fDME}} \right)}{\left[1 + 2(K_{MeOH} C_{MeOH})^{1/2} + K_{H_2O} C_{H_2O} \right]^4} \right] \quad (35)$$

In the same line, the model proposed by An et al., [210] (Table A.1) for describing the performance of CuO-ZnO-Al_2O_3-ZrO_2/HZSM-5 hybrid catalyst considered the model proposed by Graaf et al., [196,197] for methanol synthesis (Eq. (34)) the best for fitting their experimental results. Given the addition of ZrO_2 promoter to the catalyst lead to the generation of more active sites (of the same nature), the kinetic parameters established by Graaf et al., [196,197] for CZA catalysts were recalculated for CO hydrogenation to methanol (Eq. (26)), WGS (Eq. (36)), and CO_2 hydrogenation to methanol (Eq. (37)) reactions. Besides, for describing methanol dehydration these authors used the model proposed by Tao et al., [211] instead (Eq. (38)). For parameter estimation, fugacity was assumed to be equal to partial pressure and Nelder-Mead algorithm was used, achieving a good fit with an average deviation of about 6 %. Application range: 210–270 °C, 20–50 bar, SV 1000–10000 mL $g^{-1}h^{-1}$.

$$r_{rWGS} = \left[\frac{k_2 K_{CO_2} \left(f_{CO_2} f_{H_2} - \frac{f_{H_2} f_{CO}}{K_{f2}} \right)}{\left(1 + K_{CO} f_{CO} + K_{CO_2} f_{CO_2} \right) \left(f_{H_2}^{1/2} + \frac{K_{H_2O} f_{H_2O}}{K_{H_2}^{1/2}} \right)} \right] \quad (36)$$

$$r_{CO_2\ to\ MeOH} = \left[\frac{k_3 K_{CO_2} \left(f_{CO_2} f_{H_2}^{3/2} - \frac{f_{MeOH} f_{H_2O}}{f_{H_2}^{3/2} K_{f3}} \right)}{\left(1 + K_{CO} f_{CO} + K_{CO_2} f_{CO_2} \right) \left(f_{H_2}^{1/2} + \frac{K_{H_2O} f_{H_2O}}{K_{H_2}^{1/2}} \right)} \right] \quad (37)$$

$$r_{MeOH\ dehydration} = \left[\frac{k_4 \left(f_{MeOH}{}^2 - \frac{f_{DME} f_{H_2O}}{K_{f4}} \right)}{\left(1 + K'_{H_2O} f_{H_2O} + K_{MeOH} f_{MeOH} \right)} \right] \quad (38)$$

The kinetic equation established by Park et al., [212] in their model (Table A.1) differed from that proposed by Graaf et al., [196,197], and detailed elementary steps were considered for CO (Eq. (39)) and CO_2 (Eq. (40)) hydrogenation and for the adsorption of the latter. No internal or external diffusion was considered, and the adsorption equilibrium constants reported by Graaf et al., [196,197] and Ng et al., [188] were used together with the adsorption coefficient calculated for H_2O. Eq. (41) was considered for WGS reaction and an expression equivalent to Eq. (35) for methanol dehydration to DME.

$$r_{CO\ to\ MeOH} = \left[\frac{k'_A K_{CO} \left(f_{CO} f_{H_2}^{1.5} - \frac{f_{MeOH}}{f_{H_2}^{0.5} K_{P,A}} \right)}{(1 + K_{CO} f_{CO}) \left(1 + K_{H_2}^{0.5} f_{H_2}^{0.5} + K_{H_2O} f_{H_2O} \right)} \right] \quad (39)$$

$$r_{CO_2\ to\ MeOH} = \left[\frac{k'_C K_{CO_2} \left(f_{CO_2} f_{H_2}^{1.5} - \frac{f_{MeOH} f_{H_2O}}{f_{H_2}^{1.5} K_{P,C}} \right)}{\left(1 + K_{CO_2} f_{CO_2} \right) \left(1 + K_{H_2}^{0.5} f_{H_2}^{0.5} + K_{H_2O} f_{H_2O} \right)} \right] \quad (40)$$

$$r_{WGS} = \left[\frac{k'_B K_{CO_2} \left(f_{CO_2} f_{H_2}^{1.5} - \frac{f_{CO} f_{H_2O}}{K_{P,B}} \right)}{\left(1 + K_{CO_2} f_{CO_2} \right) \left(1 + K_{H_2}^{0.5} f_{H_2}^{0.5} + K_{H_2O} f_{H_2O} \right)} \right] \quad (41)$$

4.2. Specific models for the direct synthesis process

Aguayo et al., [204] proposed a kinetic model (Eqs. (42)-(45)) for the direct synthesis of DME over CuO-ZnO-Al_2O_3/γ-Al_2O_3 catalyst applicable either for H_2 + CO or H_2 + CO_2 feeds, in a wide range of operating conditions: 225–325 °C, 10–40 bar, 1.6–57 $g_{cat}\ h^{-1}\ mol_{H2}^{-1}$. In this model, methanol formation was considered to proceed through CO hydrogenation and being the rate limiting step. The WGS reaction was considered to be in equilibrium and methanol to DME dehydration considered to proceed very fast. CO_2 hydrogenation was proven to be of minor significance. That is, for H_2 + CO_2 feeds, CO_2 was believed to be previously converted to CO through the rWGS reaction. Unlike the previous models, hydrocarbons (mainly methane) formation reaction was also considered and the inhibiting effect of H_2O adsorption also taken into account with a θ term in the reaction rates of methanol formation and hydrocarbons formation. This term was related to the H_2O content by means of a hyperbolic equation (Eq. (46)), where K_{H2O} was associated to the H_2O adsorption equilibrium constant.

The same group proceeded seeking for a more accurate model widening the operating condition range and considering coke deposition on the metallic function the main responsible for catalyst deactivation (Sierra et al., [206]). The deactivation was quantified with an activity term (a) (Eq. (47)). Coke formation was proven to have oxygenates (dimethyl ether and methanol) as precursors. Consequently, the deactivation rate was quantified with an expression of the evolution of catalyst activity with time on stream, dependent on the concentration of methanol and DME (Eq. (48)), based on the hypothesis of coke formation through methoxy ion intermediates. Along with the statements proposed by Aguayo et al., [204], this model proved that the adsorption of H_2O also had an inhibiting effect on coke formation. The effect on the deactivation rate was quantified with a term θ_d related to the concentration of H_2O by the Eq. (49). Peláez et al., [213] used in their model for the direct synthesis of DME from syngas over a CuO-ZnO-Al_2O_3/γ-Al_2O_3 catalyst the Eq. (48) for the deactivation kinetic equation. As a next step for improving the kinetic model, besides the contribution of H_2O

Table 1
Operating conditions for application and main considerations of the DME synthesis kinetic models.

Catalyst	Config.	Reactor	Application range	Feedstock	Kinetic equations and considerations	Author	Ref
CuO-ZnO-Al_2O_3/ δ-Al_2O_3[a]	Dual bed	Internal-recycle	250 °C 50 bar $H_2/COx = 4$ GHSV 27500–200000 h^{-1}	$H_2 + CO + CO_2$	CO_2 to MeOH WGS MeOH to DME	Ng et al., (1999)	[188]
Cu-ZnO-Al_2O_3/ HZSM-5	Hybrid	Fluidized bed	250–270 °C 20–40 bar $H_2/CO = 0.75–2$ SV 3000 mL $g_{cat}^{-1}h^{-1}$	$H_2 + CO+ (CO_2$ trace)	CO_2 to MeOH WGS MeOH to DME	Lu et al., (2004)	[167]
Commercial MeOH synthesis[a] + MeOH dehydration[a]	Hybrid	Packed bed	220–260 °C 30–70 bar $H_2/CO = 0.8–4.6$ SV 1000 mL $g_{cat}^{-1}h^{-1}$	$H_2 + CO+ (CO_2$ trace)	CO to MeOH CO_2 to MeOH MeOH to DME	Nie et al., (2005)	[209]
Cu-ZnO-Al_2O_3/ δ-Al_2O_3	Hybrid	Packed bed	230–300 °C 8 bar $H_2/CO = 1.8$ 260–2240 g $mol^{-1}min^{-1}$	$H_2 + CO$	CO to MeOH MeOH to DME	Hadipour et al., (2008)	[189]
Cu-ZnO-Al_2O_3/ HZSM-5	Hybrid	Slurry	200–240 °C 20–50 bar $H_2/CO = 1–2$ SV 1000 mL $g_{cat}^{-1}h^{-1}$	$H_2 + CO$	CO to MeOH MeOH to DME	Moradi et al., (2008)	[156]
CuO-ZnO-Al_2O_3-ZrO_2/HZSM-5	Hybrid	Packed bed	210–270 °C 20–50 bar $H_2/CO = 3$ SV 1000–10000 mL $g_{cat}^{-1}h^{-1}$	$H_2 + CO_2$	CO to MeOH CO_2 to MeOH WGS MeOH to DME	An et al., (2008)	[210]
Cu-ZnO-Al_2O_3/ HZSM-5	Hybrid	Packed bed	220–350 °C 5–85 bar $H_2/CO_x = 0.25–3$ SV 1000–10000 mL $g_{cat}^{-1}h^{-1}$	$H_2 + CO+ (CO_2$ trace)	CO to MeOH CO_2 to MeOH WGS MeOH to DME	Shim et al., (2009)	[205]
Cu-ZnO-Al_2O_3, Süd-Chemie, MegaMax700 commercial [a]	Hybrid	Packed bed Microreactor	220–340 °C 50–90 bar $H_2/CO_x = 2–7$ $CO_2/CO_x = 0–1$ SV 8000–40000 mL $g_{cat}^{-1}h^{-1}$	$H_2 + CO + CO_2$	CO to MeOH CO_2 to MeOH WGS MeOH to DME	Park et al., (2014)	[212]
CuO-ZnO-Al_2O_3/ γ-Al_2O_3	Hybrid	Packed bed	225–325 °C 10–40 bar $H_2/CO = 2–4$ 1.6–57 g_{cat} h mol_{H2}^{-1}	$H_2 + CO$ $H_2 + CO_2$	CO to MeOH* WGS MeOH to DME HC formation*	Aguayo et al., (2007)	[204]
CuO-ZnO-Al_2O_3/ γ-Al_2O_3	Hybrid	Packed bed	225–325 °C 20–40 bar $H_2/CO = 2–4$ 0.1–68 g_{cat} h mol_C^{-1}	$H_2 + CO$	CO to MeOH*ˆ WGS MeOH to DME HC formation*	Sierra et al. (2010)	[206]
CuO-ZnO-Al_2O_3/ γ-Al_2O_3	Hybrid	Packed bed	225–325 °C 20–40 bar $H_2/CO_2 = 2–4$ 42 g_{cat} h mol_C^{-1}	$H_2 + CO_2$	CO to MeOH*+ˆ WGS MeOH to DME HC formation*+	Ereña et al. (2011)	[100]
CuO-ZnO-MnO/ SAPO-18	Hybrid	Packed bed	250–350 °C 10–40 bar $CO_2/CO_x = 0–0.5$ $H_2/CO_x = 3–4$ 1.25–20 g_{cat} h mol_C^{-1}	$H_2 + CO + CO_2$	CO to MeOH*+ˆ WGS MeOH to DME HC formation*+	Ateka et al. (2018)	[97]
CuO-ZnO-ZrO_2 @SAPO-11	Core-shell	Packed bed	250–325 °C 10–50 bar $CO_2/CO_x = 0–1$ $H_2/CO_x = 2.5–4$ 1.25–20 g_{cat} h mol_C^{-1}	$H_2 + CO + CO_2$	CO to MeOH*ˆ CO_2 to MeOH*ˆ WGS+ˆ MeOH to DMEˆ HC formation (constant)	Ateka et al. (2021)	[99]
CuO-ZnO-ZrO_2/ SAPO-11	Hybrid	Packed bed membrane reactor	275–325 °C 20–40 bar $CO_2/CO_x = 0–1$ $H_2/CO_x = 3$ 1.25–20 g_{cat} h mol_C^{-1}	$H_2 + CO + CO_2$	CO to MeOH*ˆ CO_2 to MeOH*ˆ WGS+ˆ MeOH to DME HC formation (constant)	Ateka et al. (2021)	[207]

[a] commercial catalyst.
* considering the attenuation of the reaction rate by H_2O adsorption.
+ considering the attenuation of the reaction rate by CO_2 adsorption.
ˆ Considering catalyst deactivation.

adsorption for attenuating the reaction rates, that of CO_2 adsorption was also considered by Ereña et al., [100] in the methanol and hydrocarbons formation rates, and also on deactivation (Eqs. (50) and (51), respectively). For this, the kinetic parameters were readjusted (Table A.1) for fitting experimental data obtained from H_2 + CO_2 feeds in similar reaction conditions and for equal catalysts as those used by Aguayo et al., [204].

$$r_{CO\ to\ MeOH} = k_1\left[f_{CO}f_{H_2}^2 - \frac{f_{MeOH}}{K_1}\right]\theta \tag{42}$$

$$r_{MeOH\ dehydration} = k_2\left[f_{CH_3OH}^2 - \frac{f_{MeOH}f_{H_2O}}{K_2}\right] \tag{43}$$

$$r_{rWGS} = k_3\left[f_{CO}f_{H_2O} - \frac{f_{CO_2}f_{H_2}}{K_3}\right] \tag{44}$$

$$r_{HC} = k_4\left[f_{CO}f_{H_2}^3 - \frac{f_{HC}f_{H_2O}}{K_4}\right]\theta \tag{45}$$

$$\theta = \frac{1}{1 + K_{H_2O}f_{H_2O}} \tag{46}$$

$$r_{CO\ to\ MeOH} = k_1\left[f_{CO}f_{H_2}^2 - \frac{f_{MeOH}}{K_1}\right]\theta a \tag{47}$$

$$-\frac{da}{dt} = k_d\theta_d(f_{MeOH} + f_{DME})a \tag{48}$$

$$\theta_d = \frac{1}{1 + K_{H_2O}f_{H_2O}} \tag{49}$$

$$\theta = \frac{1}{1 + K_{H_2O}f_{H_2O} + K_{CO_2}f_{CO_2}} \tag{50}$$

$$\theta_d = \frac{1}{1 + K_{H_2O,d}f_{H_2O} + K_{CO_2,d}f_{CO_2}} \tag{51}$$

Subsequently, the utilization of this model was broadened for a variety of H_2 + CO + CO_2 mixture feeds in a wide range of operating conditions using for instance CuO-ZnO-MnO/SAPO-18 hybrid catalyst [97]. An improvement of the model consisted of considering a *d* order in the deactivation kinetic equation:

$$-\frac{da}{dt} = k_d\theta_d(P_{MeOH} + P_{DME})a^d \tag{52}$$

This kinetic model was later tuned for describing the performance of a core–shell structured CuO-ZnO-ZrO_2@SAPO-11 catalyst [98]. Bearing in mind the characteristics of this catalyst, a macro-kinetic model was developed considering: i) The confinement of the individual reactions of the kinetic scheme in different regions of the catalyst particle; and ii) that the diffusion of the components through the catalyst particle influences the reaction rates [99]. At this point, in the model, methanol formation from CO (Eq. (53)) and CO_2 (Eq. (54)), rWGS (Eq. (55)), methanol dehydration (Eq. (43)) and hydrocarbon formation (Eq. (56)) reactions were considered, and the hydrocarbons formation rate was considered to be constant. It must be noted that the contribution of CO_2 to methanol formation was significant in this case. The attenuation of the WGS reaction rate by the adsorption of CO_2 was quantified with a θ_{CO_2} term defined in Eq. (57). The reactants diffusion limitation in each region of the catalyst particle was introduced (the effective diffusion coefficients are listed in Table A.1) and the concentration profile of each component determined by the expression of the mass balance considering spherical geometry (Eq. (58)). All in all, this model allowed for accurately describing the activity, quantifying the performance of CuO-ZnO-ZrO_2@SAPO-11 catalyst, and studying the influence of particle size and so, of scaling-up, on DME production and CO_2 conversion.

$$r_{CO\ to\ MeOH} = \left[k_1\left(f_{CO}f_{H_2}^2 - \frac{f_{MeOH}}{K_1}\right)\right]\theta_{H_2O}\cdot a \tag{53}$$

$$r_{CO_2\ to\ MeOH} = \left[k_4\left(f_{CO_2}f_{H_2}^3 - \frac{f_{MeOH}f_{H_2O}}{K_4}\right)\right]\theta_{H_2O}\cdot a \tag{54}$$

$$r_{rWGS} = k_3\left[f_{CO}f_{H_2O} - \frac{f_{CO_2}f_{H_2}}{K_3}\right]\theta_{CO_2}\cdot a \tag{55}$$

$$r_{HC} = \beta \tag{56}$$

$$\theta_{CO_2} = \frac{1}{1 + K_{H_2O}f_{H_2O}} \tag{57}$$

$$D_{e,i}\left(\frac{d^2y_i}{dr^2} + \frac{2}{r}\frac{dy_i}{dr}\right) = r_i\rho \tag{58}$$

It must be noted that considering the thermodynamic equilibrium is necessary in all models afore described. Bearing in mind such relevance, Behloul et al., [203] summarized the main correlations for the calculation of the equilibrium constants for the reactions of methanol synthesis, methanol dehydration and WGS, doing a comparative analysis of its application in kinetic modeling.

5. Reaction strategies and reactors for CO_2 conversion

Besides the reduced reactivity of CO_2, its conversion gives way to higher H_2O concentration. Consequently, the main advances in reactors design for the direct synthesis of DME from CO_2, or from its mixture with syngas, address the presence of H_2O in the reaction medium as the main factor limiting the thermodynamic equilibrium and the rate of the rWGS (Eq. (14)), methanol synthesis (Eqs. (15) and (18)) and methanol dehydration (Eq. (19)) reactions. Behloul et al., [203] simulated the performance of a packed bed reactor under different thermal regimes (isothermal, adiabatic and with heat transfer (shell-and-tube)) using a pseudo-homogeneous and a heterogeneous plug-flow model, with different kinetic models from the literature for the direct synthesis of DME from CO_2. Among the results, the authors stood out the importance of considering the concentration of H_2O in the kinetic model and its effect on the performance of the reactor, highlighting the relevance of a H_2O elimination strategy. As technologies for removing H_2O, reactive distillation [214], adsorption and integration of hydrophilic membranes have been proposed, among which the last two alternatives outstand.

For an overview of the reactors and strategies of interest for the direct synthesis of DME from CO_2, or from its mixture with syngas, the outstanding contributions in the literature on the strategies studied for H_2O separation by *in situ* adsorption are listed in section 5.1. In section 5.2, an analysis of the potential capacities of the different types of reactor for the direct DME synthesis process is carried out (emphasizing the H_2O removal). Section 5.3 describes the advances in the simulation and in the experimental installation of membrane reactors.

5.1. Adsorption for H_2O separation

Sorption enhanced DME synthesis (SEDMES) consists of the removal of H_2O *in situ* by a solid adsorbent. This process, like the sorption-enhanced synthesis of CO from CO_2 (SECO) and the sorption-enhanced methanol synthesis (SEMES), has a reaction-regeneration cycle [215]. A cycle comprises, a reaction and adsorption stage (in a hydrophilic zeolite mixed with the catalyst) and a stage for the regeneration of the adsorbent (using temperature swing adsorption (TSA), pressure swing adsorption or a combination of both techniques) [47]. Iliuta et al., [216] modeled the SEDMES process based on the kinetics of DME synthesis with a bifunctional Cu-ZnO-Al_2O_3/HZSM-5 catalyst and the adsorption properties of a 4A type zeolite. Among the results, an increase in CO_2 conversion up to 50 % was calculated, being 10 % without adsorbent.

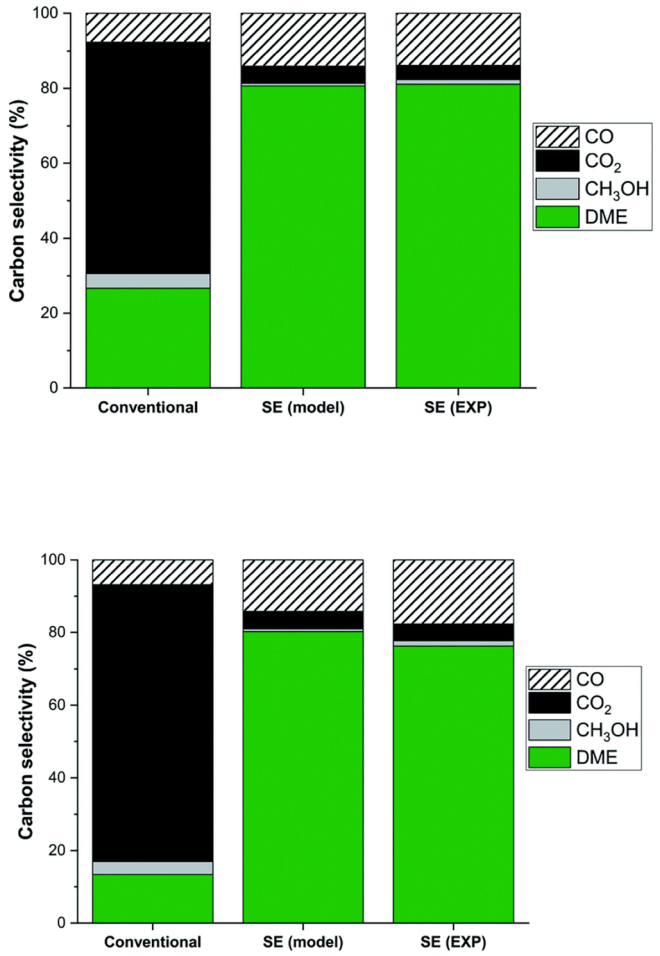

Fig. 5. Carbon selectivity for the conventional direct DME synthesis (thermodynamic equilibrium) and for sorption enhanced DME synthesis (modeled and experimental). Reproduced from the work by van Kampen et al., [217], with permission from the Royal Society of Chemistry, copyright 2021.

Van Kampen et al., [217] calculated by simulation and experimentally verified the results of the SEDMES process with a Cu-ZnO-Al_2O_3/ γ -Al_2O_3 catalyst and an LTA zeolite as adsorbent. As key factors, the optimum reaction temperature of around 250 °C, pressure above 20 bar and the catalyst to adsorbent ratio in the 1/8 to 1/4 range were established. Under these conditions, for a CO_2/CO ratio of 2, a DME selectivity of 80 % was attained (Fig. 5), with negligible catalyst deactivation [217,218]. Guffanti et al., [219] developed a heterogeneous two-dimensional dynamic model of a multitubular packed bed reactor externally cooled. The results were validated with adsorption/reaction experiments in a bench scale SEMDES packed bed reactor (2 m length, 3.8 cm internal diameter) located in the TNO facilities (Petten, Netherlands), using LTA zeolite 3A as sorbent and a bifunctional catalyst composed of CuO-ZnO-Al_2O_3 and γ -Al_2O_3. The results confirmed a high yield of DME (65–70%) in the SEMDES process. According to the prediction of the model, the CO/CO_2 ratio in the feed had little effect on the yield of DME but affected the temperature profile in the reactor. Thus, the maximum temperature in a given longitudinal position increased with increasing this ratio. However, the use of an adsorbent reduced the temperature increase due to the effect of catalyst dilution. This improves the stability of the catalyst and facilitates scaling-up, making it possible to use larger diameter reactors.

Guffanti et al [220] used the multitubular reactor simulation model to study the effect of the adsorbent/catalyst ratio, particle diameter, catalyst configuration (mechanical mixing, hybrid, core–shell) and operating variables (space velocity and pressure) on DME production and on temperature profile. Among the results, the advantage of the core–shell catalyst to moderate the maximum temperature in the reactor and therefore, to favor the stability of the catalyst stands out. In addition, the performance of the SEDMES process improved by increasing the space velocity and pressure, although these conditions required reducing the diameter of the reactor to prevent the temperature from exceeding the limit value (300 °C).

Table 2
Characteristics of different reactors for DME synthesis from CO_2.

Reactor	Advantages	Drawbacks
Packed bed (tubular)	Simple design Low cost High mass and heat transfer rate between phases Easy to integrate external membranes (tubular)	Large catalyst particle size (>1 mm) with diffusional limitations High pressure drop (lower in spherical reactor) Temperature profiles and hot spots for high conversion Gas recycling requirement for low conversion Difficulties for scaling up (using a multi-tubular reactor) Need to stop to replace deactivated catalyst and adsorbents
Slurry	Simple design Isothermal Operation in autothermic regime Catalyst circulation capacity Low pressure drop Ease of circulating H_2O adsorbents	Reduced particle size (<0.5 mm) High mechanical resistance of the catalyst required Low mass and heat transfer rate between phases Limitations of internal diffusion in the catalyst Higher volume than the tubular (packed bed) reactor in the stirred slurry Catalyst separation required (with catalyst circulation) Difficult integration of membranes to separate H_2O
Fluidized bed	Isothermal Operation in autothermic regime High mass and heat transfer rate between phases Ease of energy recovery Low pressure drop Catalyst circulation capacity Low residence time (high selectivity) Easy to scale up Easy to incorporate H_2O adsorbents	Complex equipment to operate at high pressure Reduced catalyst particle size (<1 mm) High mechanical resistance of the catalyst required Fluid dynamic limitations (gas flow restrictions) Difficult integration of membranes to separate H_2O
Micro- and structured	Higher mass and heat transfer than the conventional reactors Easy to operate with different temperature regimes Low pressure drop Low residence time (high selectivity) Flexibility to optimize different objectives High performance in ideal conditions	Difficult design and control High cost of manufacture and operation Difficult to scale up Need to stop to replace the catalyst Difficult integration of H_2O separation strategies (adsorption or membranes)

5.2. *Advantages and limitations of different reactors*

In Table 2 the advantages and drawbacks of conventional and innovative reactors are compared for the reaction from CO_2 or mixtures of CO_2 and syngas. These reactors have been studied (by simulation and experimentally) mainly with syngas feeds (section 3.3.3) and as aforementioned in this section, they require the integration of strategies to remove H_2O efficiently.

The tubular packed bed reactor is the most studied reactor due to its

simple construction and its common use in laboratory-scale experiments for kinetic modeling. Compared to other reactors, such as slurry or fluidized bed reactors, the smaller volume required for the same production is explained by the gas plug-flow approach. In addition to a simple design and low cost, the mass and heat exchange are favored by the high rate of the gas flow with respect to the catalyst. The heat removal required in this exothermal process takes place through the wall (shell-tube or shell-double tube configurations) [178].

The limitations are those inherent to packed bed reactors for exothermic reactions. Thus, large catalyst particle size (>1 mm) is required to avoid a high pressure drop. As a consequence, the limitations to intra-particle mass and heat transport are unavoidable, resulting in concentration and temperature gradients [203] and plug-flow deviations due to preferential circulation of the gas in the vicinity of the reactor wall. Moreover, longitudinal temperature profiles are generated, with the risk of generating hot spots and catalyst deactivation by sintering. To avoid these profiles, controlling the heat transmission to the outside is important, and working at low conversion values is necessary (attenuating the rate of heat generation), which requires catalyst circulation. Furthermore, the diameter of the reactor must be limited to avoid radial temperature gradients. Hence, the scale-up is carried out by arranging multiple tubes in parallel (multitubular reactor) with external cooling [165,166], with the consequent cost increase. Operating in adiabatic regime with heat exchange units between sections of the reactor allows operating with an optimal temperature profile (decreasing with the axial position) [221].

From the perspective of the use of solid adsorbents to remove the H_2O formed, the arrangement in packed beds (SEMDES process) requires periodically stopping the process to regenerate the adsorbent by means of pressure swing [217] and the catalyst by coke combustion, when necessary. Consequently, to keep DME production constant, having several multitubular reactors in operation would be necessary while one would be shut down for regeneration. However, the presence of the adsorbent together with the catalyst contributes to diminishing the maximum temperature in the reactor [219].

The tubular configuration of the packed bed reactors (with high external surface/volume ratio) is suitable for placing a hydrophilic membrane inside (with the catalyst between the membrane and the reactor wall) [222].

The arrangement of spherical packed beds, with the catalyst retained between concentric spheres, has been studied by simulation for the synthesis of methanol and for methanol dehydration to DME, using a membrane in both cases [183,223]. This reactor is also of potential interest for the direct synthesis of DME, but, although pressure drop is lower than in tubular packed beds, construction and handling costs are high. These difficulties are greater with increasing scale (requiring numerous reactors in parallel) and for operating in reaction-regeneration cycles, where loading and unloading catalyst to the reactors (and solid adsorbent if used) would be very complex tasks.

The slurry reactors can operate as CSTR (stirred reactor, easy to design and build) as in the LPDME process [224] or as bubbling bed. In both cases, the contact between gas reactants and the solid catalyst takes place in a liquid medium [225], although the CSTR requires a larger volume than the packed bed reactor, since the reactant gas flow approaches a well-mixed system. Its main advantages are the possibility to operate isothermally, in a wide range of operating conditions (particularly the CSTR) and with circulation of the catalyst. Indeed, operating in autothermal regime is possible with adequate control of the extent of the reaction. Nevertheless, the restrictions for the catalyst are important. Reduced particle size (<0.5 mm) and high mechanical resistance are required. In addition, a catalyst separation unit (by decantation) is required, for its continuous recirculation to the reactor. The fact that the relative velocity of the liquid with respect to the catalyst is very small limits the rate of mass and heat transfer between phases [226]. The scaling-up capacity is moderate, and accordingly, increasing production requires the installation of several units. The circulation of a solid for the adsorption of H_2O is feasible (with the catalyst), but this reactor is unsuitable for implementing hydrophilic membranes.

The main advantages of the fluidized bed reactor over the packed bed are the isothermal conditions, good contact between phases, low pressure drop, and ease of scale-up by catalyst circulation [227]. It is especially suitable for strongly exothermic reactions, where the generated heat can be recovered by means of heat exchangers immersed in the bed. However, the operation at high H_2 pressure limits this scaling-up for safety reasons. In this reactor, the catalyst must have high mechanical resistance to minimize the loss of material by attrition. Additionally, ideal fluid dynamics (avoiding the formation of stagnant bed zones and bubbles) require particle size being uniform, smaller than 1 mm and the gas flow being controlled at a value slightly higher than that of minimum fluidization [169]. The high velocity of the ascending gas and the random movement of the catalyst facilitate the mass and heat transfer between phases and the uniformity of the temperature in the bed, contributing (along with the small particle size) to minimize internal concentration and temperature gradients. The capacity of the fluidized reactor to operate with catalyst circulation is remarkable, and this facilitates its regeneration in a separate interconnected fluidized bed [228]. This capacity is interesting for the co-circulation of the H_2O adsorbent solid, although its separation from the catalyst at the reactor outlet would be required for the individual regeneration of both solids. A similar approach was simulated by Bayat and Asil [179] with a moving bed reactor. Conceptually, there is also potential for the integration of membranes inside the fluidized bed, which would be located perpendicularly to the distributor plate and parallel to each other (as in heat exchangers). Nevertheless, materials highly resistant to erosion would be required due to the collisions caused by the moving catalyst particles. The regeneration of these materials when saturated with H_2O would also be difficult.

There is a well-established opinion in the literature on the interest to progress in the technological development of micro-channel and structured reactors for DME synthesis based on their potential [229]. With these innovative reactors, whose study is in an incipient phase of simulation or experimentation on laboratory scale, the aim is to avoid limitations of mass and heat transport between phases, minimize pressure drop, optimize the temperature profile (adapting it to the extent of the reaction), minimize the residence time to avoid secondary reactions (methanation, rWGs, formation of hydrocarbons and coke), and increase the flexibility to address the process to the production of DME or to the conversion of CO_2. For these purposes, high mass and heat transfer between phases is achieved due to the high surface/volume ratio. It is also remarkable the capacity for the integration of the microreactors with a heat exchange unit [230], and the integration of hydrophilic membranes, combining the reaction and separation zones in the same unit [231].

5.3. Membrane reactors

The membrane reactor design is an interesting implementation within the concept of processes integration, using a selective membrane to modify the composition of the reaction medium. In this sense, the thermodynamic limitations inherent from the composition in the medium are reduced, the reaction rate and/or selectivity enhanced and, furthermore, energy requirement decreases.

Diban et al., [232] reviewed the application of membranes in catalytic reactors. Generally the catalyst was placed in a packed bed and the membrane located co-axially, with the following roles: 1) Longitudinally and selectively separating a component from the reaction medium, decreasing thereby its concentration in the medium [233]; and 2) longitudinal distribution and control of a reactant, for which the membrane is selective (reactor "crossed" flows concept). Conversely, the concentric tube with the membrane can be on the outer or the inner part of the catalytic bed. Fig. 6 shows the scheme of the two strategies for methanol synthesis with the membrane in the middle of the reactor. A hydrophilic

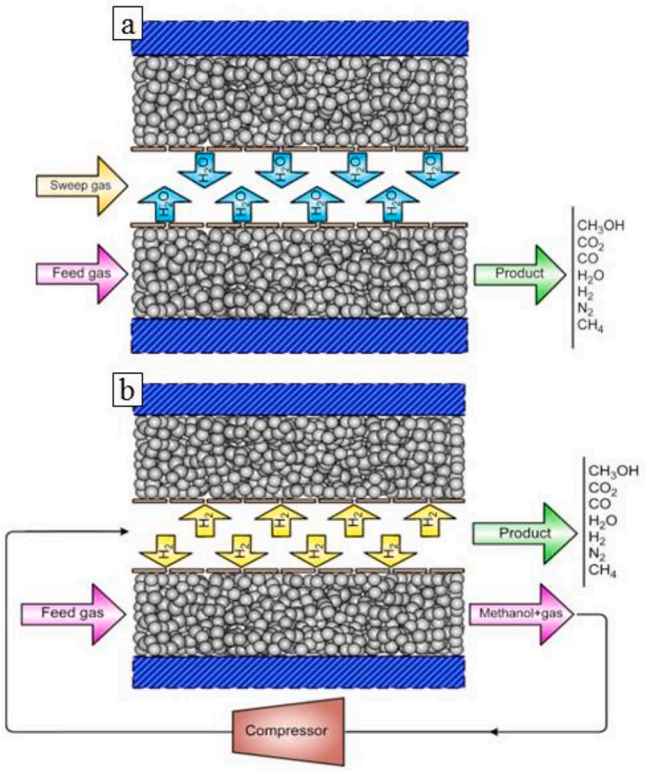

Fig. 6. Methanol synthesis schemes with H_2O (a) and H_2 (b) permselective membranes. Adapted from the work by Bayat et al., [235]. Copyright 2014, Elsevier.

membrane, H_2O permselective, which facilitates the removal of H_2O is used in Fig. 6a. In the permeate section, the H_2O formed in the reaction is continuously removed by the sweep stream (with the same composition as the reactor inlet stream), favoring the displacement of the equilibrium of methanol formation reactions [233,234]. In Fig. 6b a H_2 permselective Pd membrane is applied. Synthesis gas is injected within the catalytic bed and the gas product is compressed and recycled towards the permeation central region, allowing feeding H_2 with the suitable concentration in each longitudinal position [235]. Furthermore, Diban et al., [232] distinguished between inert and catalytic membranes (with an embedded catalyst or with catalytic activity), combining the actions of component separation and the activation of one of the reactions, in order to intensify the selective formation of products.

The use of membrane reactors in the direct synthesis of DME pursues to displace the thermodynamic equilibrium of methanol synthesis, rWGS and methanol dehydration reactions. The thermodynamic equilibrium of these reactions is disfavored by co-feeding CO_2 with synthesis gas, given the resulting higher H_2O content in the reaction medium than for syngas feeds. Consequently, a hydrophilic membrane is required to separate H_2O from the reaction medium.

5.3.1. *Hydrophilic membranes*

The main requirements to integrate a hydrophilic membrane in a catalytic reactor are: 1) Thermal stability at high temperature and under high pressure; 2) great H_2O selectivity, and; 3) high H_2O flux and permeability. H_2O permselective membranes have been extensively used in processes at low temperatures (<150 °C), in desalination, and in natural gas, air or organic compounds dehydration. Focusing on the required conditions for DME synthesis (>200 °C and high pressure), polymeric membranes have been discarded, since their performance diminishes when increasing the temperature from 50 to 200 °C (permeability from $4{\cdot}10^{-7}$ to $4{\cdot}10^{-8}$ mol s^{-1} m^{-2} Pa^{-1} and H_2O/H_2 selectivity from 150 to 18) [236]. Above 200 °C, amorphous microporous membranes (supported on ceramic materials) have moderate permeability (around 10^{-7} mol s^{-1} m^{-2} Pa^{-1}) and low H_2O/H_2 selectivity (<10) [237]. Sea and Lee [238] used a silica-alumina membrane (permeability of 10^{-7} mol s^{-1} m^{-2} Pa^{-1} and H_2O/H_2 selectivity of 8.4) in methanol dehydration towards DME, achieving a methanol conversion of 82.5 % (68 % in packed bed reactor without membrane). Nevertheless, the thermal stability of these membranes is limited.

Microporous zeolites, crystalline, with a uniform pore size, high mechanical resistance, and chemical and thermal stability are considered to be the most adequate membranes to operate above 200 °C. Moreover, with the selection of the zeolite and its composition (particularly controlling Si/Al ratio), properties such as permeability or selectivity can be modeled. H-SOD (sodalite) and MOR (mordenite) can achieve a permeability within the 10^{-7} to 10^{-6} mol s^{-1} m^{-2} Pa^{-1} range and a H_2O/H_2 selectivity higher than 10 at 250 °C [239–241], although it was tested that H-SOD had limited thermal stability above 200 °C. Fedosov et al., [242] tested a LTA membrane (NaA zeolite) for methanol dehydration towards DME, achieving a methanol conversion of 88 % (80 % without membrane) at 250 °C.

The fuel production processes wherein the utilization of zeolite membranes has received more attention, are the Fischer-Tropsch (FT) synthesis [240,243] and, to a lesser extent, the WGS reaction [244] and methanol synthesis [235]. Gallucci et al., [245] experimentally demonstrated the higher yield of methanol synthesis using a LTA membrane reactor, and Lee et al., [246] used polyamide hollow fiber membranes for the same purpose. Gorbe et al., [247] analyzed the capacity for H_2O separation of zeolite A from H_2, CO_2 and H_2O mixtures within a wide range of pressure (100–270 kPa), temperature (160–260 °C) and H_2O partial pressure, observing a remarkable limitation of this separation capacity above 240 °C.

5.3.2. *Simulation of DME synthesis in a packed bed membrane reactor*

Iliuta et al., [248] were pioneer determining the importance of the increase of CO_2 ratio in the feed on membranes efficiency, in order to favor the enhancement in methanol yield and DME selectivity, justified by the displacement of the rWGS reaction. These authors considered gas plug-flow in both reaction and permeate regions and isothermal bed

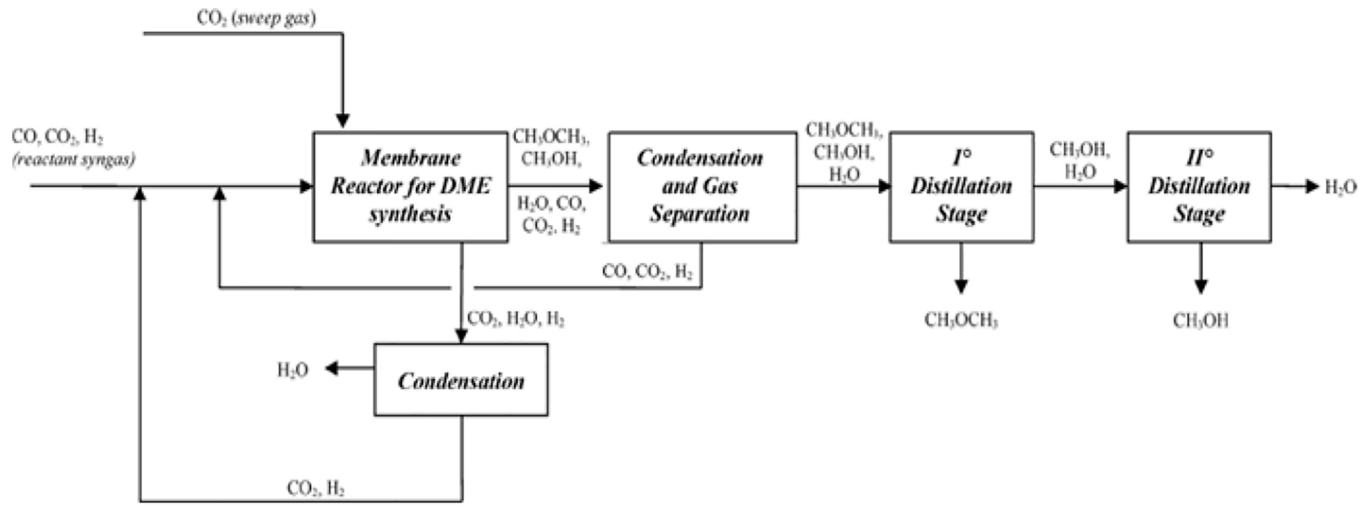

Fig. 7. Layout of the membrane reactor and the separation and recirculation units for the direct synthesis of DME (Reproduced from the work by De Falco et al., [252], copyright 2017, Elsevier).

conditions, using the kinetics of a CuO-ZnO-Al_2O_3/HZSM-5 catalyst and considering only H_2O and H_2 involved through the membrane transport.

Diban et al., [232] studied in more detail the utilization of a packed bed membrane reactor (PBMR) design model. This research study evaluated the effect of the membrane transport properties (H_2O permeability and H_2O/H_2, H_2O/CO, H_2O/CO_2, H_2O/CH_3OH, H_2O/DME, H_2O/hydrocarbons selectivity) using the kinetics of a CuO-ZnO-Al_2O_3/γ-Al_2O_3 catalyst. Gas plug-flow and isothermal reactor conditions were considered in this model. Based on HZSM-5, MOR and SIL zeolite membrane properties, an increase in CO_2 conversion of 34 % was reported. Unfortunately, the limited selectivity of these membranes decreased DME yield comparing to the values obtained without using a membrane. This decrease was due to the permeation of methanol, which can be reduced using the same reactants partial pressure both in the reaction and permeate sections. Therefore, Diban et al., [232] defined the required permeability range (for "ideal" membranes) between $0.5{\cdot}10^{-7}$ to $1.2{\cdot}10^{-7}$ mol s^{-1} m^{-2} Pa^{-1} for obtaining considerable enhancement both in CO_2 conversion and DME yield, which requires the improvement of the permeation properties of these microporous materials. The simulation allowed Diban et al., [249] to study the effect of the sweeping conditions, such as the flow (within the range from 0.06 to 1.80 mol_{CO} h^{-1}) and the gas recirculation factor ($0 < \alpha < 1$). CO_2 conversion was reported to be favored upon increasing the sweep stream flow above 0.18 mol_{CO} h^{-1}. Additionally, the need for controlling the sweep stream recirculation was reported, give its effect on DME yield, as a result of the synergy between H_2O and methanol removal from the reaction medium. Poto et al., [250] used a non-isothermal phenomenological 1D model of a PBMR to study the effect of the properties of the membrane. They established that the maximum DME yield (64 %, reached with a co-current circulation of the sweep gas) required the following membrane properties: water permeability of $4{\cdot}10^{-7}$ mol s^{-1} m^{-2} Pa^{-1}, and selectivities towards H_2, CO_2/CO and methanol of 50, 30 and 10, respectively.

Fig. 7 shows a block diagram of the membrane reactor system and CO_2 flow separation and recycling units. In this scheme proposed by De Falco et al., [251,252], condensation and gas separation systems are described. Two recirculation loops are established through a H_2O condensation unit from the permeate flow and non-condensable gases (H_2, CO_2 and CO) separation unit from the reaction flow. Methanol, DME and H_2O vapors are condensed, from which subsequently DME and methanol are successively separated in each distillation step. In the simulation of these authors a CO_2 flow in the sweeping stream was incorporated, connected to the permeate section, in contrast to the approach of Iliuta et al., [248] and Diban et al., [232,249] of maintaining the same H_2/CO_x ratio in the feed to the reaction section and the sweep stream. The equations in the model included the mass balances for the components in the reaction medium and the heat balance (different from previous models considering isothermal reactors), assuming plug-flow (1 m length and 0.038 m diameter) and used the kinetics of a CuO-ZnO-Al_2O_3/γ-Al_2O_3 catalyst [100]. The studied variables were: temperature, 200–300 °C; pressure, $5\text{-}7{\cdot}10^6$ Pa; space velocity (GHSV), up to $7{\cdot}10^3h^{-1}$; CO_2/CO_x ratio in the feed, 0.5–0.8; H_2/CO_2 ratio, 1–3; and, sweep flow (in co-current to the reaction flow). The following were determined as optimal reaction conditions: inlet temperature, 200 °C; pressure, $7{\cdot}10^6$ Pa; space velocity (GHSV), $7{\cdot}10^3h^{-1}$; CO_2/CO_x ratio in the feed, 3; H_2/CO_2 ratio, 0.7; and, sweep stream/total stream ratio, 5. At these conditions, DME yield achieved 75 % (57 % in the conventional reactor), DME selectivity 99 % (88 % in the packed bed reactor), CO_2 conversion 69 % (53 %) and CO_x conversion 75 % (65 %).

Ateka et al., [253] studied theoretically the implementation of a H-SOD membrane (with H_2O permeability of $1{\cdot}10^{-7}$ mol s^{-1} m^2 Pa^{-1} and a H_2O/H_2 selectivity of 4) in a PBMR for the direct synthesis of DME from H_2 + CO + CO_2 mixtures ranging from CO_2/CO_x 0 (that is, H_2 + CO, syngas) to 1 (H_2 + CO_2). The kinetic model previously established for a CuO-ZnO-MnO/SAPO-18 catalyst [97] was used, and various sweeping strategies where studied (N_2, H_2 and H_2 + CO + CO_2, in co-current and counter-current mode). Coinciding with Iliuta et al., [248] and Diban et al., [232,249], the best results were obtained using as sweeping stream a mixture with the same composition as that fed to the reaction section. According to the results, with this strategy a gain in CO_2 conversion between 3.5 and 5 % and DME yield ~ 25 % could be achieved over that in a packed bed reactor (PBR) (Fig. 8) [253]. These results, corresponding to per pass values, can be further improved by recycling the non-converted reactants, given this strategy (typical for industrial methanol synthesis) boosts in PBR CO_2 conversion up to 70 % and DME yield to 60 % with a recirculation factor of 0.95 (for a CO_2/CO_x ratio in the feed of 0.50, at 275 °C, 30 bar, space time of 5 g_{cat} h mol_C) [253].

Hamedi and Brinkmann [222] used a pseudo-homogeneous model to simulate the direct synthesis of DME from CO_2 in a multitubular reactor with a membrane in the wall of each tube and using H_2 as sweeping gas. Focusing the attention on the role of the membrane in the energy requirement for the reaction at 75 bar, the authors determined a reduction of 1.5%, 44.5% and 69.4% in power, heating and cooling utilities, respectively, which corresponds to a decrease of CO_2 emissions of 7.3%.

Behloul et al., [203] proposed to advance in the simulation of PBMR by considering the Damköhler numbers (a high thermal number implies a high heat transfer rate and a low separative number a deficient permeation through the membrane) to establish the optimal conditions, maximizing the synergy between the reaction, heat exchange and

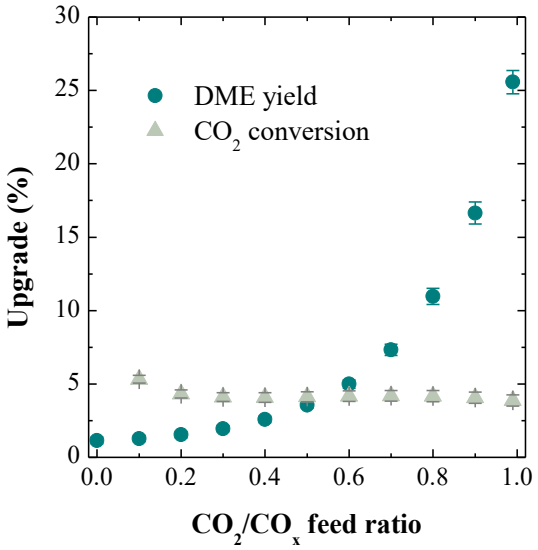

Fig. 8. Upgrade of DME yield and CO_2 conversion obtained in a PBMR reactor (using a HSOD membrane) over the results in PBR at 275 °C, 30 bar, and H_2 + CO + CO_2 mixture feeds (H_2/CO_x = 3). Adapted with permission from [253]. Copyright 2020, American Chemical Society.

membrane separation. The limitations in the mass and heat transfer in the PBR and PBMR reactors are minimized using microchannel units with a surface/volume ratio up to 50 times higher, which allows working in near-siothermal conditions, eliminating the hot spots in the reactor. Koybasi et al., [254] compared through simulation two intensified reactor systems, consisting of microchannels with the catalyst accompanied by cooling channels and adiabatic packed bed reactors in cascade with microchannel heat exchangers (cascade reactors). For certain conditions (CO_2/CO_x of 0.2, H_2/CO_x of 2, feeding at 493 °C, 50 bar and space time of 1.05 kg_{cat} s mol^{-1}), CO and CO_2 conversions and DME yield were 27. 4, 6.6 and 18.8 %, respectively, in the microchannels system; and 23.3, 4.6 and 13.8 %, respectively, in the cascade system. In addition, the lower pressure drop in the microchannels system was highlighted.

Koybasi and Avci [231] advanced in the study of process intensification by simulating the use of a SOD membrane integrated catalytic microreactor for the efficient production of DME from CO_2 containing syngas. In this approach, a membrane integrated and wall-coated catalytic microchannel reactor was presented. Differing from the former, this simulation (based on the work by Ji et al., [255]) was conducted considering the conservation of momentum and mass of the fluid phases in two dimensions (within the porous washcoat and channels, and cross-membrane) along with the chemical reactions. Membrane permeability of H_2O was assumed to be of $3{\cdot}10^{-8}$ mol m^{-2} s^{-1} Pa^{-1} based on literature information [255–257] and H_2O to H_2 permeation selectivity to remain constant (4.6) within the studied operating condition range. The cross-membrane transport of the other components in the medium was considered negligible. In the kinetic model the reaction rates defined by Vakili et al., [258] were used for CO and CO_2 hydrogenation to methanol and for methanol dehydration reactions for a Cu-ZnO-Al_2O_3/γ-Al_2O_3 catalyst, and that defined by Hu et al., [259] for the case using HZSM-5 as acidic catalyst. For computing, non-reactive transport along the gas phases of the permeate channels was assumed, while reactive transport within the catalytic zone, and laminar flow regime. Coinciding with the results of Ateka et al., with a LTA PBMR [207] (described in section 5.3.3), the achieved gain in DME production and CO_2 conversion was reported to be greater upon increasing reaction temperature within the studied 220–300 °C range. Dosing pure H_2 as permeate fluid improves CO_2 conversion and DME yield; whereas reducing permeate channel pressure, pursuing to increase the gradient of steam concentration, did not lead to positive results to Koybasi and Avci [231]. As reported, for H_2 + CO + CO_2 ternary mixtures in H_2/CO_x ratio of 2 and CO_2/CO_x ratio of 0.5 at 300 °C and 50 bar, DME yield might be improved by 11 % with using the SOD membrane, and CO_2 conversion by 20 %.

5.3.3. *Experimental PBMR system*

The suitability of using LTA membrane reactors for boosting the production of DME in a single step from CO_2 and synthesis gas mixtures was experimentally ascertained in a wide range of operating conditions (275–325 °C, 10–40 bar, $CO_2/(CO + CO_2)$ ratio in the feedstock within 0–1 range) using a CuO-ZnO-ZrO_2/SAPO-11 hybrid catalyst by Rodriguez-Vega et al., [260]. A diagram of the experimental equipment is provided in Fig. 9. The LTA membrane was selected among other

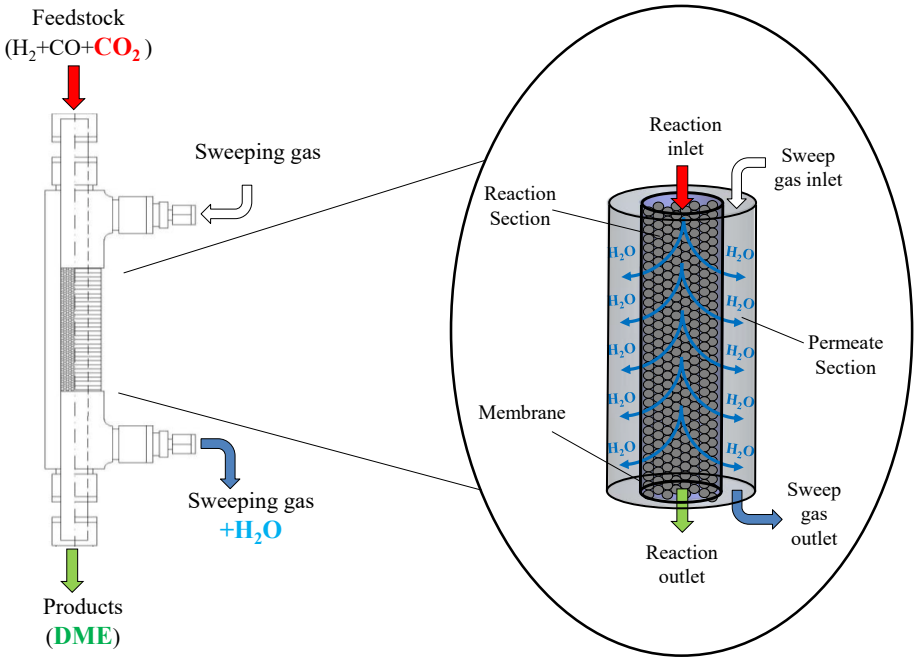

Fig. 9. Diagram of the configuration of the PBMR and component circulation. Adapted from the work by Rodriguez-Vega et al., [260], copyright 2021, Elsevier.

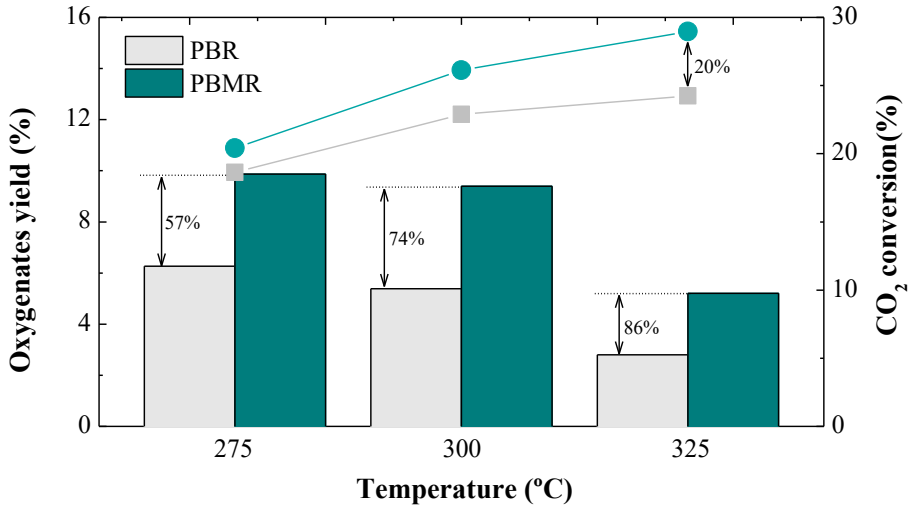

Fig. 10. Comparison of oxygenates (methanol + DME) yield and CO_2 conversion in PB and PBM reactors at 30 bar, feeding $H_2 + CO_2$ in a molar ratio of 3 and space time of 10 g_{cat} h mol_C^{-1}. Adapted from the work by Rodriguez-Vega et al., [260], copyright 2021, Elsevier.

options (LTX, SOD) regarding its permeation properties and mechanical resistance. The study revealed that, even the gas permeances were penalized at such high temperatures required for the process, the use of a LTA membrane resulted in an upgrade of 57 % on oxygenates yield (from 6.27 % for PBR to 9.87 % for PBMR) in a single pass at 275 °C and 30 bar (Fig. 10). Indeed, upon increasing reaction temperature the difference was more noticeable. At 325 °C, a gain of 86 % was achieved for oxygenates yield and of 20 % for CO_2 conversion from $H_2 + CO_2$ feeds.

These same authors established a model for the simulation of their experimental equipment. In the model the kinetics for the individual reactions were considered as described in Eqs. (43) and (53)-(56) aforementioned for the kinetic model of Ateka et al., [99]. In addition, it must be said, that besides deactivation, the effect of H_2O and CO_2 adsorption on attenuating the reaction rates activated by the metallic function (Eqs. (53)-(55)), and also on attenuating deactivation were considered (Eq. (52)). In Table A.1 (Supporting Information) the parameters used for the simulation of the PBMR are listed. The kinetic parameters were obtained in experiments without using any membrane and membrane permeability data were also experimentally determined and assumed to fit a reparameterized exponential tendency with temperature [207] (Table A.1).

The simulation of the PBMR was based on solving the convection–dispersion equation for each compound of the reaction medium and demonstrated to fit accurately the experimental data and the evolution with time on stream. Expressed as partial pressure, the one-dimension convection–dispersion equation for the concentration of each compound i in a porous catalytic bed was defined as:

$$\varepsilon \frac{\partial (P y_i)}{\partial t} = -\frac{\partial}{\partial z}\left[\upsilon P y_i - D \frac{\partial (P y_i)}{\partial z} \right] + s_i \tag{63}$$

where ε states for the effective porosity of the bed, P for total pressure, y_i for molar fraction of i compound, D for the gas effective dispersion coefficient and s_i for the source term. The linear velocity (υ) was assumed to be a function of the drop of pressure in the porous bed according to Darcy's law, and the variation of the partial pressure with time (t) and longitudinal position (z), dependant on the consumption, generation and diffusion of all gaseous compounds besides convective transport.

For the computation, a vectorized form of the conservation equations (in each section, reaction (Eq. (64)) and permeation, Eq. (65)) allowed for simultaneously modeling the chemical reaction and the deactivation of the catalyst [261]:

Reaction section:

$$\varepsilon \frac{\partial (P_R \boldsymbol{u_R})}{\partial t} = -\frac{\partial}{\partial z}\left[\upsilon P_R \frac{\partial P_R}{\partial z} \boldsymbol{u_R} \mp D \frac{\partial (P_R \boldsymbol{u_R})}{\partial z} \right] + RT\left(\rho \boldsymbol{r_c} - \frac{4}{d_R} \boldsymbol{p}^{\circ} \Delta \boldsymbol{P} \right) \tag{64}$$

Permeate section:

$$\varepsilon \frac{\partial (P_P \boldsymbol{u_P})}{\partial t} = -\frac{\partial}{\partial z}\left[\upsilon P_P \frac{\partial P_P}{\partial z} \boldsymbol{u_P} \mp D \frac{\partial (P_P \boldsymbol{u_P})}{\partial z} \right] + RT \frac{4}{d_R} \boldsymbol{p}^{\circ} \Delta \boldsymbol{P} \tag{65}$$

where $\boldsymbol{u_R}$ and $\boldsymbol{u_P}$ state for vectors of dependent variables for the reaction and permeate sections, respectively; P_R and P_P to the total pressure in the reaction and permeate sections, respectively (bar); $\boldsymbol{p}$ for the vector of permeances of the i compounds (mol m^{-2} h^{-1} bar^{-1}); $\boldsymbol{r_c}$ for the vector containing the reaction rates of each component i and deactivation rate; $\Delta \boldsymbol{P}$ for the vector of pressure differences between the reaction and permeate sections for each i component (bar); and d_R for the diameter of the reactor (m).

Note that in both sections, the source term considered the diffusion of the compounds from one section to the other, and for the reaction section, the generation by chemical reaction was also taken into account. Therefore, the simulation results fit the experimental results (Fig. 11) and provided plenty information on the process proceeding. Using the model for simulation, a maximum DME yield of 68 % was reported for synthesis gas feeds, and surpassed 5 % for $CO_2 + H_2$ at 325 °C and 40 bar, reaching a 17 % of CO_2 conversion for ternary mixtures of $H_2 + CO_2/CO$ in the feed ($CO_2/CO_x = 0.5$).

6. Challenges and perspectives

Dieterich et al., [221] made a review gathering the commercial technologies for DME synthesis in one- or two-stages, developed for syngas feeds. Some technologies for the two-stage synthesis (Haldor Topsøe, Lurgi, Toyo Engineering Corporation (TEC), Mitsubishi Gas Chemical, Johnson Matthey) are based on methanol synthesis, to which a packed bed reactor for the methanol dehydration stage is incorporated. More recent ones, marketed by Chinese companies (China Energy, Tianyi, ENN), address methanol recycling.

The direct synthesis of DME has been developed on pilot plant scale with different technologies. Thus, Haldor Topsøe's technology is based on that of methanol synthesis but using bifunctional catalysts. These catalysts are placed in a multitubular reactor (packed beds with external cooling) in the technology of Korea Gas Corporation (KOGAS). Other companies (Japanese Corporation JFE (NKK), Air products and Chemicals Inc.) use stirred slurry reactors due to the heat transfer capabilities. The scaling limit of this reactor (considered 100 ton day^{-1}) can be

increased with a bubbly flow. Unitel Technologies in Australia (https://www.uniteltech.com) has developed the use of liquidized reactors with the challenge of adapting their fluid dynamics to operate under high pressure.

The direct synthesis of DME is also receiving renewed interest from other companies (Linde AG, BASF SE) for the prospects of CO_2 upgrading. The implementation of this process is conditioned by the need for scientific and technological advances in the development of catalyst, kinetic modeling and design of new reactors. The kinetic modeling faces the challenge of comprising the characteristics of a complex reaction scheme under specific reaction conditions (different from those of methanol synthesis and dehydration), where the presence of H_2O (at higher concentration than in the direct synthesis of DME from syngas) plays a relevant role: i) As a reactant displacing the thermodynamic equilibrium of methanol synthesis and dehydration; ii) attenuating the activity of the metallic and acid sites of the catalyst; iii) promoting deactivation by sintering of the metallic sites and; iv) attenuating coke deposition. Consequently, considering the role of H_2O in the deactivation mechanism and in the kinetic modeling is necessary [97,100,204,262]. For the process scale-up, it is important to point out the relevance of quantifying the deactivation of the catalyst with kinetics considering different causes and the corresponding mechanism. In addition, for quantifying adequately the deactivation kinetics, the kinetic models must be established using rigorous data analysis methodologies of results obtained in long time on stream (TOS) experiments in reactors with well-defined flows.

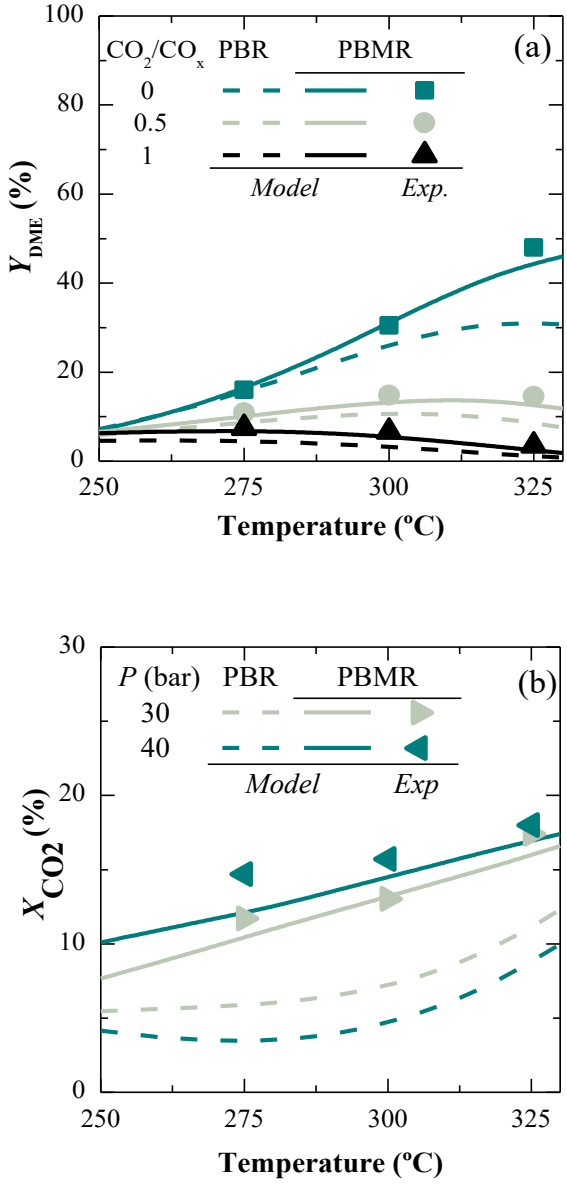

Fig. 11. Comparison of DME yield (a) and CO_2 conversion (b) obtained in a PBMR with LTA membrane and in a PBR. Operating conditions: 30 bar; space time 10 g_{cat} h mol_C^{-1}; feed composition, H_2/CO_x = 3 and CO_2/CO_x = 0.5. Reproduced from the work by Ateka et al., [207], copyright 2021, Elsevier.

The technological development of the direct synthesis of DME from CO_2 also relies on the remarkable knowledge on the reactor design strategies for its synthesis from syngas (section 3.3.3). Thereby, the lower reaction heat when co-feeding CO_2 together with syngas [95] is an advantage for using a bench of adiabatic packed bed reactors in series or a multitubular reactor externally cooled (technologies developed for methanol synthesis). However, the relevance of the presence of H_2O on limiting the thermodynamics and hydrogenation kinetics, leads to the conclusion that the development of the membrane reactor is a priority alternative. The progress in the development of membrane reactors simulation models is important and the potential of these reactors to shift the thermodynamic equilibrium of the reactions of methanol and DME synthesis, WGS and methanol dehydration has been well established in the literature [232,248,249,251–253]. In addition, the advances in the preparation of hydrophilic ceramic membranes are remarkable, and the capacity of a LTA zeolite membrane in this process has been experimentally verified [207,260]. However, there are important challenges for the industrial implementation of this technology. Among these: i) Improving the properties of the membranes, H_2O permselectivity in particular; ii) developing pilot- and demonstration plant- scale equipment to facilitate research conducting long-term experiments and optimizing sweeping strategies. Although the per-pass conversion with the membrane reactor is much higher than that obtained in conventional packed bed reactors, the need for recirculation of the non-reacted gas stream ($CO + CO_2 + H_2$) must also be considered. By means of simulation models, it has been verified that the advantages of the microchannel reactors, that is, favoring the mass and heat transfer between phases (discussed in section 3.3.3 for syngas feeds), are also interesting for the direct synthesis of DME from CO_2 together with syngas [263,264]. The simulation results of the integration of supported sodalite (SOD) membranes in a micro-channel reactor are also interesting as DME yield of 17 % and CO_2 conversion of 15.8 % can be achieved dosing pure H_2 as permeate gas [231].

The future of the direct synthesis of DME from CO_2 also depends on socio-economic aspects surrounding the activities of the energy sector. In particular, the availability of H_2 obtained with renewable energies is crucial for the viability of the process. However, to the current high costs of water electrolysis (partially mature technology [265,266]), the technical difficulties inherent to H_2 transport and to the safety of its handling at high pressure (due to the hazard of explosion in the presence of air) must be added [267]. In this sense, the integration of processes for the production of DME from methane can play an important role, feeding directly into the synthesis reactor the stream generated in the methane tri-reforming (with CO_2, O_2 and steam) [268]. The production of hydrogen from biomass, by means of bio-oil reforming or directly by on-line pyrolysis-reforming [269]) is specially interesting in the short and medium term to be integrated with gasification, in order to obtain an adequate H_2/CO_x ratio for DME synthesis with biomass as only source of carbon and hydrogen.

Another determining factor for the economic viability of DME as fuel and as a raw material for the production of hydrocarbons (fuels and chemicals as light olefins and BTX aromatics) is the value of these products in their corresponding markets. The qualities of DME as a fuel for domestic use, in the automotive industry and in steam generating boilers have been widely proven (Section 3). It is a “green” fuel obtained

from sustainable sources, easy to handle and with high cetane number. DME is therefore one of the "green" candidates for replacing conventional fuels and the relevance of its implementation in the fuel market will be conditioned by the competition within the energy sector for the replacement of petroleum derivatives. With well-defined specifications, and whose commercialization could be carried out using the current LPG distribution facilities. Its use as fuel, when obtained by co-feeding syngas derived from non-edible biomass, represents a sustainable valorization route of lower technological difficulty than directly using bio-oil as a fuel, which requires expensive physical and thermochemical treatment stages.

A fundamental feature of the DME economy is its relationship with the CO_2 economy. Hence, it is noteworthy that in the direct synthesis of DME, the production of DME and the conversion of CO_2 have opposite evolutions. The optimal operating conditions for DME production correspond to a CO_2/CO ratio below 1/3 and for boosting CO_2 conversion values above 3 are adequate [262]. This requires establishing intermediate operating conditions to achieve a balanced compromise between both objectives. That is, obtaining high yield of DME with net conversion of CO_2. Furthermore, the progressive increase in CO_2 emission taxes will be a determining factor for the economy of the process, suggesting to increase the CO_2 content in the feed, favoring its conversion.

Besides, the technology for DME production (although not completely mature, as shown in this review) only has some minor additional difficulties compared to the already mature technology of methanol synthesis (including those related to the co-feeding of CO_2 in high concentration together with the syngas). The use of DME as a raw material for the production of light olefins, aromatics or gasoline offers good prospects. DME (with a greater capacity to generate methyl oxonium species on Brønsted sites) is more active than methanol for the production of light olefins [76], and allows using HZSM-5 as catalyst (with slower coke deactivation than industrially used SAPO-34 in the MTO (methanol-to-olefins) process) [74]. Therefore, the industrial implementation of the DTO (DME-to-olefins) process could be carried out using the mature technology of the MTO process, consisting of an interconnected reactor-regenerator system (fluidized bed) [228]. Likewise, the implementation of DME steam reforming technology for the production of H_2 for fuel cells is a mature technology [83,270], with advantages over the valorization of other oxygenates (as bio-oil, bioethanol or glycerol), inherent to the properties of DME (Section 3). Based on this capacity, DME is considered a H_2 vector, the production of which can be a suitable way to "store" renewable energies in periods of production excess [83].

7. Conclusions

During the last two decades the interest of DME production in one step, using bifunctional catalysts, has increased with the perspective of valorizing CO_2. Moreover, the perspectives of using DME as "green" fuel, raw material for the production of light olefins or aromatics and as H_2 vector are promising, and consequently, these reactions are receiving great attention, and new catalysts, kinetic models and reactors are being developed.

The direct synthesis of DME offers thermodynamic advantages over methanol synthesis and is more energy efficient and of lower production cost than either methanol synthesis or the two-step synthesis of DME. These advantages favor the conversion of CO_2 and its co-feeding with syngas. The requirement of a moderate H_2/CO_x ratio makes feasible using syngas derived from the gasification of biomass and wastes as feed.

In particular, it has aroused the need for performing significant innovations in the catalyst, kinetic modeling and in the reactor design, due to the effect of co-feeding CO_2 on the conversion, selectivity and stability of the catalyst, and in the decrease of the yields in comparison to the values obtained from synthesis gas feeds.

The challenges in the direct synthesis of DME when feeding CO_2 are related to two particular factors conditioning the process: i) The low reactivity of CO_2 hydrogenation, and; ii) the increase of H_2O content in the reaction medium with respect to using syngas feeds, being WGS reaction displaced, and consequently, disfavoring methanol synthesis and dehydration reactions. Furthermore, H_2O is adsorbed in the metallic sites of the catalyst decreasing their activity and, additionally, favoring the irreversible deactivation (by sintering) of these sites. The activity of the acid sites also diminishes, to a greater extent when the acidic function is hydrophilic. Therefore, as to overcome these limitations a great deal of effort has been placed in two lines: i) On the catalysts, tailoring conventional catalysts and proposing new alternatives and configurations, that seek to favor the synergy of the proximity of the methanol synthesis and dehydration reactions, minimizing deactivation, and; ii) on the operation, developing new reaction strategies and reactor designs. For which developing kinetic models, capable for a precise description of the performance of the process with the applied catalyst and in a wide range of operating conditions is very helpful.

The kinetic models developed combining those established in the literature for the synthesis of methanol and its dehydration, offer good performance in literature studies to predict products yields in the direct synthesis of DME with CO_2 in the feed, although the original models were proposed for optimal conditions (temperature, pressure) for each of these stages, and generally for methanol synthesis from syngas.

Considering that the suitable conditions for the direct synthesis of DME are different (intermediate temperature and pressure) from those suitable for each of the two stages integrated, new kinetic models have been proposed. These models were also based on LHHW premises, and their validity has been tested for different conventional catalysts, with hybrid and core–shell configurations.

For a more accurate simulation of the process, it is important to consider in the kinetic model the deactivation of the catalyst (mainly by coke) and the concentration of H_2O in the reaction medium, since the adsorption of the latter attenuates the activity of the metallic and acid sites. Moreover, the role of H_2O must be considered also in the deactivation kinetics, as it contributes to attenuate the deactivation by coke, by inhibiting the condensation of its precursors.

To overcome the thermodynamic limitation of CO_2 conversion, different strategies for the *in situ* adsorption of H_2O in the reactor have been studied. However, the effectiveness of these strategies is conditioned by their difficult experimental implementation on a large scale. Membrane reactors are crucial for the industrial implementation of DME synthesis, since H_2O can be selectively separated using hydrophilic membranes. Different theoretical works have established simulation programs for these reactors, but the experimental implementation relies on the difficulty of not having a membrane with the required stability at the severe pressure and temperature conditions used in the process. In this sense, the results obtained with a packed bed reactor and an LTA zeolite membrane are encouraging.

The level of knowledge achieved in the fundamental aspects (collected in this review) allows considering that the CO_2 to DME synthesis process can effectively contribute to the mitigation of climate change. Even if the state of the required technology is more mature than that of other alternatives for the catalytic upgrading of CO_2, achieving the necessary challenges for this objective requires a multidisciplinary work at different scales (catalyst, kinetic modeling, reactor design and scaling).

CRediT authorship contribution statement

A. Ateka: Conceptualization, Methodology, Investigation, Data curation, Writing – original draft, Writing – review & editing. **P. Rodriguez-Vega:** Investigation, Writing – original draft. **J. Ereña:** Writing – original draft. **A.T. Aguayo:** Project administration, Conceptualization, Supervision. **J. Bilbao:** Conceptualization, Methodology, Investigation, Data curation, Writing – original draft, Writing – review & editing, Supervision.

Declaration of Competing Interest

The authors declare that they have no known competing financial interests or personal relationships that could have appeared to influence the work reported in this paper.

Acknowledgements

This work has been carried out with the financial support of the Ministry of Science, Innovation and Universities of the Spanish Government (PID2019-108448RB-100); the Basque Government (Project IT1645-22); the European Regional Development Funds (ERDF); and the European Commission (HORIZON H2020-MSCA RISE-2018. Contract No. 823745).

Appendix A. Supplementary data

The kinetic equations discussed in Section 4 and the corresponding kinetic parameters have been gathered in Table A.1. Supplementary data to this article can be found online at https://doi.org/10.1016/j.fuel.2022.125148.

References

[1] International Energy Agency I. Global Energy Review 2021 – Analysis - IEA 2021. https://www.iea.org/reports/global-energy-review-2021 (accessed November 2, 2021).
[2] International Energy Agency I. Net Zero by 2050 – Analysis - IEA 2021. https://www.iea.org/reports/net-zero-by-2050 (accessed November 2, 2021).
[3] Ahmad T, Zhang D. A critical review of comparative global historical energy consumption and future demand: The story told so far. Energy Rep 2020;6:1973–91. https://doi.org/10.1016/J.EGYR.2020.07.020.
[4] Tao L, Choksi TS, Liu W, Pérez-Ramírez J. Synthesizing high-volume chemicals from CO_2 without direct H_2 input. ChemSusChem 2020;13:6066–89. https://doi.org/10.1002/CSSC.202001604.
[5] Dragone G, Kerssemakers AAJ, Driessen JLSP, Yamakawa CK, Brumano LP, Mussatto SI. Innovation and strategic orientations for the development of advanced biorefineries. Bioresour Technol 2020;302:122847. https://doi.org/10.1016/J.BIORTECH.2020.122847.
[6] Wang C, Zhang X, Liu Q, Zhang Q, Chen L, Ma L. A review of conversion of lignocellulose biomass to liquid transport fuels by integrated refining strategies. Fuel Process Technol 2020;208:106485. https://doi.org/10.1016/J.FUPROC.2020.106485.
[7] Palos R, Gutiérrez A, Vela FJ, Olazar M, Arandes JM, Bilbao J. Waste refinery: the valorization of waste plastics and end-of-life tires in refinery units. A Review Energy & Fuels 2021;35:3529–57. https://doi.org/10.1021/ACS.ENERGYFUELS.0C03918.
[8] (Global CCS Institute). Facilities - Global CCS Institute 2021. https://co2re.co/FacilityData (accessed November 2, 2021).
[9] Bachu S. Review of CO_2 storage efficiency in deep saline aquifers. Int J Greenh Gas Control 2015;40:188–202. https://doi.org/10.1016/J.IJGGC.2015.01.007.
[10] Cao C, Liu H, Hou Z, Mehmood F, Liao J, Feng W. A review of CO_2 storage in view of safety and cost-effectiveness. Energies 2020;13:600. https://doi.org/10.3390/EN13030600.
[11] Assen AH, Belmabkhout Y, Adil K, Lachehab A, Hassoune H, Aggarwal H. Advances on CO_2 storage. Synthetic porous solids, mineralization and alternative solutions. Chem Eng J 2021;419:129569.
[12] Dutta A, Farooq S, Karimi IA, Khan SA. Assessing the potential of CO_2 utilization with an integrated framework for producing power and chemicals. J CO2 Util 2017;19:49–57. https://doi.org/10.1016/J.JCOU.2017.03.005.
[13] Rafiee A, Rajab Khalilpour K, Milani D, Panahi M. Trends in CO_2 conversion and utilization: A review from process systems perspective. J Environ Chem Eng 2018;6:5771–94. https://doi.org/10.1016/j.jece.2018.08.065.
[14] Chen G, Waterhouse GIN, Shi R, Zhao J, Li Z, Wu LZ, et al. From solar energy to fuels: recent advances in light-driven C1 chemistry. Angew Chemie - Int Ed 2019;58:17528–51. https://doi.org/10.1002/anie.201814313.
[15] Aresta M, Dibenedetto A, Quaranta E. State of the art and perspectives in catalytic processes for CO_2 conversion into chemicals and fuels: The distinctive contribution of chemical catalysis and biotechnology. J Catal 2016;343:2–45. https://doi.org/10.1016/J.JCAT.2016.04.003.
[16] Grim RG, Huang Z, Guarnieri MT, Ferrell JR, Tao L, Schaidle JA. Transforming the carbon economy: challenges and opportunities in the convergence of low-cost electricity and reductive CO_2 utilization. Energy Environ Sci 2020;13:472–94. https://doi.org/10.1039/C9EE02410G.
[17] Zhang Z, Pan SY, Li H, Cai J, Olabi AG, Anthony EJ, et al. Recent advances in carbon dioxide utilization. Renew Sustain Energy Rev 2020;125:109799. https://doi.org/10.1016/J.RSER.2020.109799.
[18] Salehizadeh H, Yan N, Farnood R. Recent advances in microbial CO_2 fixation and conversion to value-added products. Chem Eng J 2020;390:124584. https://doi.org/10.1016/J.CEJ.2020.124584.
[19] Mustafa A, Lougou BG, Shuai Y, Wang Z, Tan H. Current technology development for CO_2 utilization into solar fuels and chemicals: A review. J Energy Chem 2020;49:96–123. https://doi.org/10.1016/J.JECHEM.2020.01.023.
[20] Godin J, Liu W, Ren S, Xu CC. Advances in recovery and utilization of carbon dioxide: A brief review. J Environ Chem Eng 2021;9(4):105644.
[21] Kamkeng ADN, Wang M, Hu J, Du W, Qian F. Transformation technologies for CO_2 utilisation: Current status, challenges and future prospects. Chem Eng J 2021;409:128138. https://doi.org/10.1016/j.cej.2020.128138.
[22] Naims H. Economics of carbon dioxide capture and utilization—a supply and demand perspective. Environ Sci Pollut Res 2016;23:22226–41. https://doi.org/10.1007/S11356-016-6810-2.
[23] Alper E, Yuksel OO. CO_2 utilization: Developments in conversion processes. Petroleum 2017;3:109–26. https://doi.org/10.1016/j.petlm.2016.11.003.
[24] Zheng Y, Zhang W, Li Y, Chen J, Yu B, Wang J, et al. Energy related CO_2 conversion and utilization: Advanced materials/nanomaterials, reaction mechanisms and technologies. NANO Energy 2017;40:512–39. https://doi.org/10.1016/J.NANOEN.2017.08.049.
[25] Jarvis SM, Samsatli S. Technologies and infrastructures underpinning future CO_2 value chains: A comprehensive review and comparative analysis. Renew Sustain Energy Rev 2018;85:46–68. https://doi.org/10.1016/J.RSER.2018.01.007.
[26] Norhasyima RS, Mahlia TMI. Advances in CO_2 utilization technology: A patent landscape review. J CO2 Util 2018;26:323–35. https://doi.org/10.1016/J.JCOU.2018.05.022.
[27] Centi G, Quadrelli EA, Perathoner S. Catalysis for CO_2 conversion: a key technology for rapid introduction of renewable energy in the value chain of chemical industries. Energy Environ Sci 2013;6:1711–31. https://doi.org/10.1039/C3EE00056G.
[28] Arinaga AM, Ziegelski MC, Marks TJ. Alternative Oxidants for the Catalytic Oxidative Coupling of Methane. Angew Chemie Int Ed 2021;60:10502–15. https://doi.org/10.1002/ANIE.202012862.
[29] Al-Shafei EN, Robert Brown D, Katikaneni SP, Aljama H, H. Al-Badairy H. Direct conversion of CO_2 with methane into chemicals over ZrO_2/TiO_2 catalysts. Chem Eng J 2021;419:129416.
[30] Najari S, Saeidi S, Concepcion P, Dionysiou DD, Bhargava SK, Lee AF, et al. Oxidative dehydrogenation of ethane: catalytic and mechanistic aspects and future trends. Chem Soc Rev 2021;50:4564–605. https://doi.org/10.1039/D0CS01518K.
[31] Jiang X, Sharma L, Fung V, Park SJ, Jones CW, Sumpter BG, et al. Oxidative Dehydrogenation of Propane to Propylene with Soft Oxidants via Heterogeneous Catalysis. ACS Catal 2021;11:2182–234. https://doi.org/10.1021/ACSCATAL.0C03999.
[32] Song K, Wang S, Sun Q, Xu D. Study of oxidative dehydrogenation of ethylbenzene with CO_2 on supported CeO_2-Fe_2O_3 binary oxides. Arab J Chem 2020;13:7357–69. https://doi.org/10.1016/J.ARABJC.2020.08.013.
[33] Wang L, Wang Y, Zhang R, Ding R, Chen X, Lv B. Edge-Activating CO_2-Mediated Ethylbenzene Dehydrogenation by a Hierarchical Porous BN Catalyst. ACS Catal 2020;10:6697–706. https://doi.org/10.1021/ACSCATAL.0C00070.
[34] Jung S, Lee J, Moon DH, Kim KH, Kwon EE. Upgrading biogas into syngas through dry reforming. Renew Sustain Energy Rev 2021;143:110949. https://doi.org/10.1016/J.RSER.2021.110949.
[35] Li Z, Lin Q, Li M, Cao J, Liu F, Pan H, et al. Recent advances in process and catalyst for CO_2 reforming of methane. Renew Sustain Energy Rev 2020;134:110312. https://doi.org/10.1016/J.RSER.2020.110312.
[36] Wang C, Wang Y, Chen M, Liang D, Yang Z, Cheng W, et al. Recent advances during CH_4 dry reforming for syngas production: A mini review. Int J Hydrogen Energy 2021;46:5852–74. https://doi.org/10.1016/J.IJHYDENE.2020.10.240.
[37] Shafiqah MNN, Tran HN, Nguyen TD, Phuong PTT, Abdullah B, Lam SS, et al. Ethanol CO_2 reforming on La_2O_3 and CeO_2-promoted Cu/Al_2O_3 catalysts for enhanced hydrogen production. Int J Hydrogen Energy 2020;45:18398–410. https://doi.org/10.1016/J.IJHYDENE.2019.10.024.
[38] Mohd Arif NN, Abidin SZ, Osazuwa OU, Vo DVN, Azizan MT, Taufiq-Yap YH. Hydrogen production via CO_2 dry reforming of glycerol over ReNi/CaO catalysts. Int J Hydrogen Energy 2019;44:20857–71. https://doi.org/10.1016/J.IJHYDENE.2018.06.084.
[39] Yu B, Diao ZF, Guo CX, He LN. Carboxylation of olefins/alkynes with CO_2 to industrially relevant acrylic acid derivatives. J CO2 Util 2013;1:60–8. https://doi.org/10.1016/J.JCOU.2013.01.001.
[40] Honda M, Tamura M, Nakagawa Y, Sonehara S, Suzuki K, Fujimoto K, et al. Ceria-Catalyzed Conversion of Carbon Dioxide into Dimethyl Carbonate with 2-Cyanopyridine. ChemSusChem 2013;6:1341–4. https://doi.org/10.1002/CSSC.201300229.
[41] Jutz F, Grunwaldt JD, Baiker A. In situ XAS study of the Mn(III)(salen)Br catalyzed synthesis of cyclic organic carbonates from epoxides and CO_2. J Mol Catal A Chem 2009;297:63–72. https://doi.org/10.1016/J.MOLCATA.2008.10.009.
[42] Xiang X, Guo L, Wu X, Ma X, Xia Y. Urea formation from carbon dioxide and ammonia at atmospheric pressure. Environ Chem Lett 2012;10:295–300. https://doi.org/10.1007/S10311-012-0366-2.
[43] Ye R-P, Ding J, Gong W, Argyle MD, Zhong Q, Wang Y, et al. CO_2 hydrogenation to high-value products via heterogeneous catalysis. Nat Commun 2019;10:1–15. https://doi.org/10.1038/s41467-019-13638-9.

[44] Modak A, Bhanja P, Dutta S, Chowdhury B, Bhaumik A. Catalytic reduction of CO_2 into fuels and fine chemicals. Green Chem 2020;22:4002–33. https://doi.org/10.1039/D0GC01092H.

[45] Atsbha TA, Yoon T, Seongho P, Lee C-J. A review on the catalytic conversion of CO_2 using H_2 for synthesis of CO, methanol, and hydrocarbons. J CO2 Util 2021;44:101413.

[46] Saeidi S, Najari S, Hessel V, Wilson K, Keil FJ, Concepción P, et al. Recent advances in CO_2 hydrogenation to value-added products — Current challenges and future directions. Prog Energy Combust Sci 2021;85:100905. https://doi.org/10.1016/j.pecs.2021.100905.

[47] Vu TTN, Desgagnés A, Iliuta MC. Efficient approaches to overcome challenges in material development for conventional and intensified CO_2 catalytic hydrogenation to CO, methanol, and DME. Appl Catal A Gen 2021;617:118119. https://doi.org/10.1016/j.apcata.2021.118119.

[48] Wang W, Wang S, Ma X, Gong J. Recent advances in catalytic hydrogenation of carbon dioxide. Chem Soc Rev 2011;40:3703–27. https://doi.org/10.1039/c1cs15008a.

[49] Li J, Wang L, Cao Y, Zhang C, He P, Li H. Recent advances on the reduction of CO_2 to important C_{2+} oxygenated chemicals and fuels. Chinese J Chem Eng 2018;26:2266–79. https://doi.org/10.1016/J.CJCHE.2018.07.008.

[50] Hussain I, Jalil AA, Hassan NS, Hamid MYS. Recent advances in catalytic systems for CO_2 conversion to substitute natural gas (SNG): Perspective and challenges. J Energy Chem 2021;62:377–407. https://doi.org/10.1016/J.JECHEM.2021.03.040.

[51] Lee WJ, Li C, Prajitno H, Yoo J, Patel J, Yang Y, et al. Recent trend in thermal catalytic low temperature CO_2 methanation: A critical review. Catal Today 2021;368:2–19. https://doi.org/10.1016/J.CATTOD.2020.02.017.

[52] Faria AC, Miguel CV, Rodrigues AE, Madeira LM. Modeling and Simulation of a Steam-Selective Membrane Reactor for Enhanced CO_2 Methanation. Ind Eng Chem Res 2020;59:16170–84. https://doi.org/10.1021/ACS.IECR.0C02860.

[53] Iwakiri IGI, Faria AC, Miguel CV, Madeira LM. Split feed strategy for low-permselective membrane reactors: A simulation study for enhancing CO_2 methanation. Chem Eng Process - Process Intensif 2021;163:108360. https://doi.org/10.1016/J.CEP.2021.108360.

[54] Ferri D, Bürgi T, Baiker A. Probing boundary sites on a Pt/Al_2O_3 model catalyst by CO_2 hydrogenation and in situ ATR-IR spectroscopy of catalytic solid–liquid interfaces. Phys Chem Chem Phys 2002;4:2667–72. https://doi.org/10.1039/B111498K.

[55] Pajares A, Prats H, Romero A, Viñes F, de la Piscina PR, Sayós R, et al. Critical effect of carbon vacancies on the reverse water gas shift reaction over vanadium carbide catalysts. Appl Catal B Environ 2020;267:118719. https://doi.org/10.1016/J.APCATB.2020.118719.

[56] Yan B, Zhao B, Kattel S, Wu Q, Yao S, Su D, et al. Tuning CO_2 hydrogenation selectivity via metal-oxide interfacial sites. J Catal 2019;374:60–71. https://doi.org/10.1016/J.JCAT.2019.04.036.

[57] Guil-López R, Mota N, Llorente J, Millán E, Pawelec B, Fierro JLG, et al. Methanol Synthesis from CO_2: A Review of the Latest Developments in Heterogeneous Catalysis. Materials (Basel) 2019;12:3902. https://doi.org/10.3390/MA12233902.

[58] Jiang X, Nie X, Guo X, Song C, Chen JG. Recent Advances in Carbon Dioxide Hydrogenation to Methanol via Heterogeneous Catalysis. Chem Rev 2020;120:7984–8034. https://doi.org/10.1021/acs.chemrev.9b00723.

[59] Zhang S, Wu Z, Liu X, Hua K, Shao Z, Wei B, et al. A Short Review of Recent Advances in Direct CO_2 Hydrogenation to Alcohols. Top Catal 2021;64:371–94. https://doi.org/10.1007/S11244-020-01405-W.

[60] Zhang X, Zhang G, Song C, Guo X. Catalytic Conversion of Carbon Dioxide to Methanol: Current Status and Future Perspective. Front Energy Res 2021;8:621119. https://doi.org/10.3389/FENRG.2020.621119.

[61] Zhong J, Yang X, Wu Z, Liang B, Huang Y, Zhang T. State of the art and perspectives in heterogeneous catalysis of CO_2 hydrogenation to methanol. Chem Soc Rev 2020;49:1385–413. https://doi.org/10.1039/c9cs00614a.

[62] Tountas AA, Peng X, Tavasoli AV, Duchesne PN, Dingle TL, Dong Y, et al. Towards Solar Methanol: Past, Present, and Future. Adv Sci 2019;6:1801903. https://doi.org/10.1002/advs.201801903.

[63] Yang C, Mu R, Wang G, Song J, Tian H, Zhao Z-J, et al. Hydroxyl-mediated ethanol selectivity of CO_2 hydrogenation. Chem Sci 2019;10:3161–7. https://doi.org/10.1039/C8SC05608K.

[64] Saeidi S, Najari S, Fazlollahi F, Nikoo MK, Sefidkon F, Klemeš JJ, et al. Mechanisms and kinetics of CO_2 hydrogenation to value-added products: A detailed review on current status and future trends. Renew Sustain Energy Rev 2017;80:1292–311. https://doi.org/10.1016/j.rser.2017.05.204.

[65] Tan L, Zhang P, Cui Y, Suzuki Y, Li H, Guo L, et al. Direct CO_2 hydrogenation to light olefins by suppressing CO by-product formation. Fuel Process Technol 2019;196:106174. https://doi.org/10.1016/j.fuproc.2019.106174.

[66] Ramirez A, Chowdhury AD, Dokania A, Cnudde P, Caglayan M, Yarulina I, et al. Effect of Zeolite Topology and Reactor Configuration on the Direct Conversion of CO_2 to Light Olefins and Aromatics. ACS Catal 2019;9:6320–34. https://doi.org/10.1021/acscatal.9b01466.

[67] Wei J, Ge Q, Yao R, Wen Z, Fang C, Guo L, et al. Directly converting CO_2 into a gasoline fuel. Nat Commun 2017;8:1–9. https://doi.org/10.1038/ncomms15174.

[68] Semelsberger TA, Borup RL, Greene HL. Dimethyl ether (DME) as an alternative fuel. J Power Sources 2006;156:497–511. https://doi.org/10.1016/j.jpowsour.2005.05.082.

[69] Arcoumanis C, Bae C, Crookes R, Kinoshita E. The potential of di-methyl ether (DME) as an alternative fuel for compression-ignition engines: A review. Fuel 2008;87:1014–30. https://doi.org/10.1016/j.fuel.2007.06.007.

[70] Azizi Z, Rezaeimanesh M, Tohidian T, Rahimpour MR. Dimethyl ether: A review of technologies and production challenges. Chem Eng Process Process Intensif 2014;82:150–72. https://doi.org/10.1016/j.cep.2014.06.007.

[71] Khalifi M, Zirrahi M, Hassanzadeh H, Abedi J. Concentration-dependent molecular diffusion coefficient of dimethyl ether in bitumen. Fuel 2020;274:117809. https://doi.org/10.1016/J.FUEL.2020.117809.

[72] Fleisch TH, Basu A, Sills RA. Introduction and advancement of a new clean global fuel: The status of DME developments in China and beyond. J Nat Gas Sci Eng 2012;9:94–107. https://doi.org/10.1016/j.jngse.2012.05.012.

[73] Ying W, Longbao Z, Hewu W. Diesel emission improvements by the use of oxygenated DME/diesel blend fuels. Atmos Environ 2006;40:2313–20. https://doi.org/10.1016/J.ATMOSENV.2005.12.016.

[74] Tian P, Wei Y, Ye M, Liu Z. Methanol to olefins (MTO): From fundamentals to commercialization. ACS Catal 2015;5:1922–38. https://doi.org/10.1021/acscatal.5b00007.

[75] Khadzhiev SN, Kolesnichenko NV, Ezhova NN. Manufacturing of lower olefins from natural gas through methanol and its derivatives (review). Pet Chem 2008;48:325–34. https://doi.org/10.1134/S0965544108050010.

[76] Cordero-Lanzac T, Martínez C, Aguayo AT, Castaño P, Bilbao J, Corma A. Activation of n-pentane while prolonging HZSM-5 catalyst lifetime during its combined reaction with methanol or dimethyl ether. Catal Today 2020;383:320–9. https://doi.org/10.1016/j.cattod.2020.09.015.

[77] Pérez-Uriarte P, Ateka A, Aguayo AT, Gayubo AG, Bilbao J. Kinetic model for the reaction of DME to olefins over a HZSM-5 zeolite catalyst. Chem Eng J 2016;302:801–10. https://doi.org/10.1016/j.cej.2016.05.096.

[78] Ibáñez M, Pérez-Uriarte P, Sánchez-Contador M, Cordero-Lanzac T, Aguayo AT, Bilbao J, et al. Nature and Location of Carbonaceous Species in a Composite HZSM-5 Zeolite Catalyst during the Conversion of Dimethyl Ether into Light Olefins. Catalysts 2017;7:254–66. https://doi.org/10.3390/catal7090254.

[79] Cordero-Lanzac T, Aguayo AT, Gayubo AG, Bilbao J. Consideration of the activity distribution using the population balance theory for designing a dual fluidized bed reactor-regenerator system. Application to the MTO process. Chem Eng J 2021;405:126448.

[80] Oar-Arteta L, Remiro A, Epron F, Bion N, Aguayo AT, Bilbao J, et al. Comparison of Noble Metal- and Copper-Based Catalysts for the Step of Methanol Steam Reforming in the Dimethyl Ether Steam Reforming Process. Ind Eng Chem Res 2016;55:3546–55. https://doi.org/10.1021/acs.iecr.6b00126.

[81] Zhang TQ, Choi B, Kim YB. Numerical and experimental study on hydrogen production via dimethyl ether steam reforming. Int J Hydrogen Energy 2020;45:11438–48. https://doi.org/10.1016/J.IJHYDENE.2020.02.091.

[82] Su X, Zhang F, Yin Y, Tu B, Cheng M. Thermodynamic analysis of fuel composition and effects of different dimethyl ether processing technologies on cell efficiency. Fuel Process Technol 2020;203:106391. https://doi.org/10.1016/J.FUPROC.2020.106391.

[83] Catizzone E, Freda C, Braccio G, Frusteri F, Bonura G. Dimethyl ether as circular hydrogen carrier: Catalytic aspects of hydrogenation/dehydrogenation steps. J Energy Chem 2021;58:55–77. https://doi.org/10.1016/j.jechem.2020.09.040.

[84] Catizzone E, Bonura G, Migliori M, Frusteri F, Giordano G. CO_2 Recycling to Dimethyl Ether: State-of-the-Art and Perspectives. Molecules 2017;23:31. https://doi.org/10.3390/MOLECULES23010031.

[85] Schemme S, Breuer JL, Köller M, Meschede S, Walman F, Samsun RC, et al. H_2-based synthetic fuels: A techno-economic comparison of alcohol, ether and hydrocarbon production. Int J Hydrogen Energy 2020;45:5395–414. https://doi.org/10.1016/J.IJHYDENE.2019.05.028.

[86] Kim SM, Lee YJ, Bae JW, Potdar HS, Jun KW. Synthesis and characterization of a highly active alumina catalyst for methanol dehydration to dimethyl ether. Appl Catal A Gen 2008;348:113–20. https://doi.org/10.1016/J.APCATA.2008.06.032.

[87] Hosseini Z, Taghizadeh M, Yaripour F. Synthesis of nanocrystalline γ-Al_2O_3 by sol-gel and precipitation methods for methanol dehydration to dimethyl ether. J Energy Chem 2011;20:128–34. https://doi.org/10.1016/S1003-9953(10)60172-7.

[88] Zuo Z, Huang W, Han P, Gao Z, Li Z. Theoretical studies on the reaction mechanisms of AlOOH- and γ-Al_2O_3-catalysed methanol dehydration in the gas and liquid phases. Appl Catal A Gen 2011;408:130–6. https://doi.org/10.1016/J.APCATA.2011.09.011.

[89] Kim SD, Baek SC, Lee YJ, Jun KW, Kim MJ, Yoo IS. Effect of γ-alumina content on catalytic performance of modified ZSM-5 for dehydration of crude methanol to dimethyl ether. Appl Catal A Gen 2006;309:139–43. https://doi.org/10.1016/J.APCATA.2006.05.008.

[90] Zeng L, Wang Y, Mou J, Liu F, Yang C, Zhao T, et al. Promoted catalytic behavior over γ-Al_2O_3 composited with ZSM-5 for crude methanol conversion to dimethyl ether. Int J Hydrogen Energy 2020;45:16500–8. https://doi.org/10.1016/J.IJHYDENE.2020.04.115.

[91] Catizzone E, Aloise A, Migliori M, Giordano G. The effect of FER zeolite acid sites in methanol-to-dimethyl-ether catalytic dehydration. J Energy Chem 2017;26:406–15. https://doi.org/10.1016/j.jechem.2016.12.005.

[92] Catizzone E, Aloise A, Giglio E, Ferrarelli G, Bianco M, Migliori M, et al. MFI vs. FER zeolite during methanol dehydration to dimethyl ether: The crystal size plays a key role. Catal Commun 2021;149:106214.

[93] Chen W-H, Hsu C-L, Wang X-D. Thermodynamic approach and comparison of two-step and single step DME (dimethyl ether) syntheses with carbon dioxide utilization. Energy 2016;109:326–40. https://doi.org/10.1016/j.energy.2016.04.097.

[94] Olah GA, Goeppert A, Prakash GKS. Chemical recycling of carbon dioxide to methanol and dimethyl ether: From greenhouse gas to renewable,

environmentally carbon neutral fuels and synthetic hydrocarbons. J Org Chem 2009;74:487–98. https://doi.org/10.1021/jo801260f.
[95] Ateka A, Pérez-Uriarte P, Gamero M, Ereña J, Aguayo AT, Bilbao J. A comparative thermodynamic study on the CO_2 conversion in the synthesis of methanol and of DME. Energy 2017;120:796–804. https://doi.org/10.1016/j.energy.2016.11.129.
[96] Dadgar F, Myrstad R, Pfeifer P, Holmen A, Venvik HJ. Catalyst Deactivation During One-Step Dimethyl Ether Synthesis from Synthesis Gas. Catal Lett 2017.865–79.;2017(1474):147. https://doi.org/10.1007/S10562-017-1971-2.
[97] Ateka A, Ereña J, Bilbao J, Aguayo AT. Kinetic modeling of the direct synthesis of dimethyl ether over a CuO-ZnO-MnO/SAPO-18 catalyst and assessment of the CO_2 conversion. Fuel Process Technol 2018;181:233–43. https://doi.org/10.1016/j.fuproc.2018.09.024.
[98] Ateka A, Sánchez-Contador M, Portillo A, Bilbao J, Aguayo AT. Kinetic modeling of CO_2+CO hydrogenation to DME over a CuO-ZnO-ZrO_2@SAPO-11 core-shell catalyst. Fuel Process Technol 2020;206:106434–44. https://doi.org/10.1016/j.fuproc.2020.106434.
[99] Ateka A, Portillo A, Sánchez-Contador M, Bilbao J, Aguayo AT. Macro-kinetic model for CuO–ZnO–ZrO_2@SAPO-11 core-shell catalyst in the direct synthesis of DME from CO/CO_2. Renew Energy 2021;169:1242–51. https://doi.org/10.1016/j.renene.2021.01.062.
[100] Ereña J, Sierra I, Aguayo AT, Ateka A, Olazar M, Bilbao J. Kinetic modelling of dimethyl ether synthesis from (H_2+CO_2) by considering catalyst deactivation. Chem Eng J 2011;174:660–7. https://doi.org/10.1016/j.cej.2011.09.067.
[101] Sierra I, Ereña J, Aguayo AT, Arandes JM, Olazar M, Bilbao J. Co-feeding water to attenuate deactivation of the catalyst metallic function (CuO–ZnO–Al_2O_3) by coke in the direct synthesis of dimethyl ether. Appl Catal B Environ 2011;106:167–73. https://doi.org/10.1016/j.apcatb.2011.05.021.
[102] Li Z, Li J, Dai M, Liu Y, Han D, Wu J. The effect of preparation method of the Cu–La_2O_3–ZrO_2/γ-Al_2O_3 hybrid catalysts on one-step synthesis of dimethyl ether from syngas. Fuel 2014;121:173–7. https://doi.org/10.1016/j.fuel.2013.12.050.
[103] Oyola-Rivera O, Baltanás MA, Cardona-Martínez N. CO_2 hydrogenation to methanol and dimethyl ether by Pd–Pd_2Ga catalysts supported over Ga_2O_3 polymorphs. J CO2 Util 2015;9:8–15. https://doi.org/10.1016/j.jcou.2014.11.003.
[104] Qin Z, Zhou X, Su T, Jiang Y, Ji H. Hydrogenation of CO_2 to dimethyl ether on La-, Ce-modified Cu-Fe/HZSM-5 catalysts. Catal Commun 2016;75:78–82. https://doi.org/10.1016/j.catcom.2015.12.010.
[105] Zhou X, Su T, Jiang Y, Qin Z, Ji H, Guo Z. CuO-Fe_2O_3-CeO_2/HZSM-5 bifunctional catalyst hydrogenated CO_2 for enhanced dimethyl ether synthesis. Chem Eng Sci 2016;153:10–20. https://doi.org/10.1016/j.ces.2016.07.007.
[106] Ateka A, Pérez-Uriarte P, Sánchez-Contador M, Ereña J, Aguayo AT, Bilbao J. Direct synthesis of dimethyl ether from syngas on CuO-ZnO-MnO/SAPO-18 bifunctional catalyst. Int J Hydrogen Energy 2016;41(40):18015–26.
[107] Sánchez-Contador M, Ateka A, Rodriguez-Vega P, Bilbao J, Aguayo AT. Optimization of the Zr Content in the CuO-ZnO-ZrO_2/SAPO-11 Catalyst for the Selective Hydrogenation of CO+CO_2 Mixtures in the Direct Synthesis of Dimethyl Ether. Ind Eng Chem Res 2018;57:1169–78. https://doi.org/10.1021/acs.iecr.7b04345.
[108] Ateka A, Sierra I, Ereña J, Bilbao J, Aguayo AT. Performance of CuO–ZnO–ZrO_2 and CuO–ZnO–MnO as metallic functions and SAPO-18 as acid function of the catalyst for the synthesis of DME co-feeding CO_2. Fuel Process Technol 2016;152:34–45. https://doi.org/10.1016/j.fuproc.2016.05.041.
[109] Frusteri F, Cordaro M, Cannilla C, Bonura G. Multifunctionality of Cu–ZnO–ZrO_2/H-ZSM5 catalysts for the one-step CO_2-to-DME hydrogenation reaction. Appl Catal B Environ 2015;162:57–65. https://doi.org/10.1016/j.apcatb.2014.06.035.
[110] Jiang X, Koizumi N, Guo X, Song C. Bimetallic Pd–Cu catalysts for selective CO_2 hydrogenation to methanol. Appl Catal B Environ 2015;170–171:173–85. https://doi.org/10.1016/J.APCATB.2015.01.010.
[111] Arena F, Barbera K, Italiano G, Bonura G, Spadaro L, Frusteri F. Synthesis, characterization and activity pattern of Cu–ZnO/ZrO_2 catalysts in the hydrogenation of carbon dioxide to methanol. J Catal 2007;249:185–94. https://doi.org/10.1016/J.JCAT.2007.04.003.
[112] Li M-M-J, Zeng Z, Liao F, Hong X, Tsang SCE. Enhanced CO_2 hydrogenation to methanol over CuZn nanoalloy in Ga modified Cu/ZnO catalysts. J Catal 2016;343:157–67. https://doi.org/10.1016/J.JCAT.2016.03.020.
[113] Sanguineti PB, Baltanás MA, Bonivardi AL. Copper–gallia interaction in Cu–Ga_2O_3–ZrO_2 catalysts for methanol production from carbon oxide(s) hydrogenation. Appl Catal A Gen 2015;504:476–81. https://doi.org/10.1016/J.APCATA.2014.11.021.
[114] Xiao J, Mao D, Guo X, Yu J. Methanol Synthesis from CO_2 Hydrogenation over CuO–ZnO–TiO_2 Catalysts: The Influence of TiO_2 Content. Energy Technol 2015;3:32–9. https://doi.org/10.1002/ENTE.201402091.
[115] Pasupulety N, Driss H, Alhamed YA, Alzahrani AA, Daous MA, Petrov L. Studies on Au/Cu–Zn–Al catalyst for methanol synthesis from CO_2. Appl Catal A Gen 2015;504:308–18. https://doi.org/10.1016/J.APCATA.2015.01.036.
[116] Martin O, Mondelli C, Curulla-Ferré D, Drouilly C, Hauert R, Pérez-Ramírez J. Zinc-Rich Copper Catalysts Promoted by Gold for Methanol Synthesis. ACS Catal 2015;5:5607–16. https://doi.org/10.1021/ACSCATAL.5B00877.
[117] Pasupulety N, Driss H, Alhamed YA, Alzahrani AA, Daous MA, Petrov L. Influence of preparation method on the catalytic activity of Au/Cu-Zn-Al catalyst for CO_2 hydrogenation to methanol. Chim Cinétique Catal 2015:1511–8. https://doi.org/10.1007/978-3-319-61112-9_1.
[118] Fierro JLG, Melián-Cabrera I, López GM. Reverse Topotactic Transformation of a Cu–Zn–Al Catalyst during Wet Pd Impregnation: Relevance for the Performance in Methanol Synthesis from CO_2/H_2 Mixtures. J Catal 2002;210:273–84. https://doi.org/10.1006/JCAT.2002.3676.
[119] Melián-Cabrera I, Granados ML, Fierro JLG. Pd-Modified Cu–Zn Catalysts for Methanol Synthesis from CO_2/H_2 Mixtures: Catalytic Structures and Performance. J Catal 2002;210:285–94. https://doi.org/10.1006/jcat.2002.3677.
[120] Choi EJ, Lee YH, Lee DW, Moon DJ, Lee KY. Hydrogenation of CO_2 to methanol over Pd–Cu/CeO_2 catalysts. Mol Catal 2017;434:146–53. https://doi.org/10.1016/J.MCAT.2017.02.005.
[121] Liu L, Fan F, Bai M, Xue F, Ma X, Jiang Z, et al. Mechanistic study of methanol synthesis from CO_2 hydrogenation on Rh-doped Cu(111) surfaces. Mol Catal 2019;466:26–36. https://doi.org/10.1016/J.MCAT.2019.01.009.
[122] Zhang C, Liao P, Wang H, Sun J, Gao P. Preparation of novel bimetallic CuZn-BTC coordination polymer nanorod for methanol synthesis from CO_2 hydrogenation. Mater Chem Phys 2018;215:211–20. https://doi.org/10.1016/J.MATCHEMPHYS.2018.05.028.
[123] Wang J, Li G, Li Z, Tang C, Feng Z, An H, et al. A highly selective and stable ZnO-ZrO_2 solid solution catalyst for CO_2 hydrogenation to methanol. Sci Adv 2017;3:e1701290.
[124] Chen TY, Cao C, Chen TB, Ding X, Huang H, Shen L, et al. Unraveling Highly Tunable Selectivity in CO_2 Hydrogenation over Bimetallic In-Zr Oxide Catalysts. ACS Catal 2019;9:8785–97. https://doi.org/10.1021/acscatal.9b01869.
[125] Wang J, Zhang G, Zhu J, Zhang X, Ding F, Zhang A, et al. CO_2 Hydrogenation to Methanol over In_2O_3-Based Catalysts: From Mechanism to Catalyst Development. ACS Catal 2021;11:1406–23. https://doi.org/10.1021/acscatal.0c03665.
[126] Ghosh S, Sebastian J, Olsson L, Creaser D. Experimental and kinetic modeling studies of methanol synthesis from CO_2 hydrogenation using In_2O_3 catalyst. Chem Eng J 2021;416:129120. https://doi.org/10.1016/j.cej.2021.129120.
[127] Stangeland K, Kalai DY, Ding Y, Yu Z. Mesoporous manganese-cobalt oxide spinel catalysts for CO_2 hydrogenation to methanol. J CO2 Util 2019;32:146–54. https://doi.org/10.1016/J.JCOU.2019.04.018.
[128] Rui N, Wang Z, Sun K, Ye J, Ge Q, Liu C, et al. CO_2 hydrogenation to methanol over Pd/In_2O_3: effects of Pd and oxygen vacancy. Appl Catal B Environ 2017;218:488–97. https://doi.org/10.1016/J.APCATB.2017.06.069.
[129] Ojelade OA, Zaman SF, Daous MA, Al-Zahrani AA, Malik AS, Driss H, et al. Optimizing Pd: Zn molar ratio in PdZn/Ce_O2 for C_O2 hydrogenation to methanol. Appl Catal A Gen 2019;584:117185. https://doi.org/10.1016/J.APCATA.2019.117185.
[130] Li C-S, Melaet G, Ralston WT, An K, Brooks C, Ye Y, et al. High-performance hybrid oxide catalyst of manganese and cobalt for low-pressure methanol synthesis. Nat Commun 2015;6:1–5. https://doi.org/10.1038/ncomms7538.
[131] Bahruji H, Bowker M, Hutchings G, Dimitratos N, Wells P, Gibson E, et al. Pd/ZnO catalysts for direct CO_2 hydrogenation to methanol. J Catal 2016;343:133–46. https://doi.org/10.1016/J.JCAT.2016.03.017.
[132] Bahruji H, Bowker M, Jones W, Hayward J, Esquius JR, Morgan DJ, et al. PdZn catalysts for CO_2 hydrogenation to methanol using chemical vapour impregnation (CVI). Faraday Discuss 2017;197:309–24. https://doi.org/10.1039/C6FD00189K.
[133] Martin O, Martín AJ, Mondelli C, Mitchell S, Segawa TF, Hauert R, et al. Indium Oxide as a Superior Catalyst for Methanol Synthesis by CO_2 Hydrogenation. Angew Chemie Int Ed 2016;55:6261–5. https://doi.org/10.1002/ANIE.201600943.
[134] Liu D, Yao C, Zhang J, Fang D, Chen D. Catalytic dehydration of methanol to dimethyl ether over modified γ-Al_2O_3 catalyst. Fuel 2011;90:1738–42. https://doi.org/10.1016/J.FUEL.2011.01.038.
[135] Sun X, Mueller S, Liu Y, Shi H, Haller GL, Sanchez-Sanchez M, et al. On reaction pathways in the conversion of methanol to hydrocarbons on HZSM-5. J Catal 2014;317:185–97. https://doi.org/10.1016/J.JCAT.2014.06.017.
[136] Catizzone E, Aloise A, Migliori M, Giordano G. Dimethyl ether synthesis via methanol dehydration: Effect of zeolite structure. Appl Catal A Gen 2015;502:215–20. https://doi.org/10.1016/j.apcata.2015.06.017.
[137] Catizzone E, Giglio E, Migliori M, Cozzucoli PC, Giordano G. The effect of zeolite features on the dehydration reaction of methanol to dimethyl ether: Catalytic behaviour and kinetics. Materials (Basel) 2020;13:1–15. https://doi.org/10.3390/ma13235577.
[138] Ereña J, Garoña R, Arandes JM, Aguayo AT, Bilbao J. Effect of operating conditions on the synthesis of dimethyl ether over a CuO-ZnO-Al_2O_3/NaHZSM-5 bifunctional catalyst. Catal Today 2005;107–108:467–73. https://doi.org/10.1016/j.cattod.2005.07.116.
[139] Vanoye L, Favre-Réguillon A, Munno P, Rodríguez JF, Dupuy S, Pallier S, et al. Methanol dehydration over commercially available zeolites: Effect of hydrophobicity. Catal Today 2013;215:239–42. https://doi.org/10.1016/j.cattod.2013.01.012.
[140] Sánchez-Contador M, Ateka A, Aguayo AT, Bilbao J. Behavior of SAPO-11 as acid function in the direct synthesis of dimethyl ether from syngas and CO_2. J Ind Eng Chem 2018;63:245–54. https://doi.org/10.1016/j.jiec.2018.02.022.
[141] Aloise A, Marino A, Dalena F, Giorgianni G, Migliori M, Frusteri L, et al. Desilicated ZSM-5 zeolite: Catalytic performances assessment in methanol to DME dehydration. Microporous Mesoporous Mater 2020;302:110198. https://doi.org/10.1016/J.MICROMESO.2020.110198.
[142] Aboul-Fotouh SMK, Ali LI, Naghmash MA, Aboul-Gheit NAK. Effect of the Si/Al ratio of HZSM-5 zeolite on the production of dimethyl ether before and after ultrasonication. J Fuel Chem Technol 2017;45:581–8. https://doi.org/10.1016/S1872-5813(17)30030-0.
[143] Chen Z, Li X, Xu Y, Dong Y, Lai W, Fang W, et al. Fabrication of nano-sized SAPO-11 crystals with enhanced dehydration of methanol to dimethyl ether. Catal Commun 2018;103:1–4. https://doi.org/10.1016/j.catcom.2017.09.002.

[144] Frusteri F, Migliori M, Cannilla C, Frusteri L, Catizzone E, Aloise A, et al. Direct CO_2-to-DME hydrogenation reaction: New evidences of a superior behaviour of FER-based hybrid systems to obtain high DME yield. J CO2 Util 2017;18:353–61. https://doi.org/10.1016/j.jcou.2017.01.030.

[145] Catizzone E, Aloise A, Migliori M, Giordano G. From 1-D to 3-D zeolite structures: performance assessment in catalysis of vapour-phase methanol dehydration to DME. Microporous Mesoporous Mater 2017;243:102–11. https://doi.org/10.1016/j.micromeso.2017.02.022.

[146] Ateka A, Rodriguez-Vega P, Ereña J, Aguayo AT, Bilbao J. A review on the valorization of CO_2. Focusing on the thermodynamics and catalyst design studies of the direct synthesis of dimethyl ether. Fuel Process Technol 2022;233:107310.

[147] Ateka A, Sánchez-Contador M, Ereña J, Aguayo AT, Bilbao J. Catalyst configuration for the direct synthesis of dimethyl ether from CO and CO_2 hydrogenation on CuO–ZnO–MnO/SAPO-18 catalysts. React Kinet Mech Catal 2018;124:401–18. https://doi.org/10.1007/s11144-018-1344-x.

[148] Bonura G, Cordaro M, Spadaro L, Cannilla C, Arena F, Frusteri F. Hybrid Cu–ZnO–ZrO_2/H-ZSM5 system for the direct synthesis of DME by CO_2 hydrogenation. Appl Catal B Environ 2013;140–141:16–24. https://doi.org/10.1016/j.apcatb.2013.03.048.

[149] García-Trenco A, Martínez A. The influence of zeolite surface-aluminum species on the deactivation of CuZnAl/zeolite hybrid catalysts for the direct DME synthesis. Catal Today 2014;227:144–53. https://doi.org/10.1016/j.cattod.2013.09.051.

[150] Phienluphon R, Pinkaew K, Yang G, Li J, Wei Q, Yoneyama Y, et al. Designing core (Cu/ZnO/Al_2O_3)–shell (SAPO-11) zeolite capsule catalyst with a facile physical way for dimethyl ether direct synthesis from syngas. Chem Eng J 2015;270:605–11. https://doi.org/10.1016/j.cej.2015.02.071.

[151] Guffanti S, Visconti CG, Groppi G. Model Analysis of the Effects of Active Phase Distribution at the Pellet Scale in Catalytic Reactors for the Direct Dimethyl Ether Synthesis. Ind Eng Chem Res 2020;59:14252–66. https://doi.org/10.1021/acs.iecr.0c01938.

[152] Sánchez-Contador M, Ateka A, Aguayo AT, Bilbao J. Direct synthesis of dimethyl ether from CO and CO_2 over a core-shell structured CuO-ZnO-ZrO_2@SAPO-11 catalyst. Fuel Process Technol 2018;179:258–68. https://doi.org/10.1016/j.fuproc.2018.07.009.

[153] Sánchez-Contador M, Ateka A, Ibáñez M, Bilbao J, Aguayo AT. Influence of the operating conditions on the behavior and deactivation of a CuO-ZnO-ZrO_2@SAPO-11 core-shell-like catalyst in the direct synthesis of DME. Renew Energy 2019;138:585–97. https://doi.org/10.1016/j.renene.2019.01.093.

[154] Mondal U, Yadav GD. Perspective of dimethyl ether as fuel_ Part II- analysis of reactor systems and industrial processes. J CO2 Util 2019;32:321–38. https://doi.org/10.1016/j.jcou.2019.02.006.

[155] Zhang L, Bian Z, Sun K, Huang W. Effects of Sn on the catalytic performance for one step syngas to DME in slurry reactor. New J Chem 2021;45:3783–9. https://doi.org/10.1039/D0NJ05195K.

[156] Moradi GR, Ahmadpour J, Yaripour F. Intrinsic kinetics study of LPDME process from syngas over bi-functional catalyst. Chem Eng J 2008;144:88–95. https://doi.org/10.1016/j.cej.2008.05.018.

[157] Lin J, Han M, Wang T, Zhang T, Wang J, Jin Y. Influence of the gas distributor on the local hydrodynamic behavior of an external loop airlift reactor. Chem Eng J 2004;102:51–9. https://doi.org/10.1016/J.CEJ.2004.01.023.

[158] Bakopoulos A. Multiphase fluidization in large-scale slurry jet loop bubble columns for methanol and or dimethyl ether production. Chem Eng Sci 2006;61:538–57. https://doi.org/10.1016/J.CES.2005.06.035.

[159] Moradi GR, Ghanei R, Yaripour F. Determination of the optimum operating conditions for direct synthesis of dimethyl ether from syngas. Int J Chem React Eng 2007;5. https://doi.org/10.2202/1542-6580.1367/MACHINEREADABLECITATION/RIS.

[160] Papari S, Kazemeini M, Fattahi M. Mathematical modeling of a slurry reactor for DME direct synthesis from syngas. J Nat Gas Chem 2012;21:148–57. https://doi.org/10.1016/S1003-9953(11)60347-2.

[161] Papari S, Kazemeini M, Fattahi M, Fatahi M. DME direct synthesis from syngas in a large-scale three-phase slurry bubble column reactor: transitient modeling. Chem Eng Commun 2014;201:612–34. https://doi.org/10.1080/00986445.2013.782292.

[162] Li Z, Zuo Z, Huang W, Xie K. Research on Si–Al based catalysts prepared by complete liquid-phase method for DME synthesis in a slurry reactor. Appl Surf Sci 2011;257:2180–3. https://doi.org/10.1016/J.APSUSC.2010.09.069.

[163] Yagi H, Ohno Y, Inoue N, Okuyama K, Aoki S. Slurry phase reactor technology for DME direct synthesis. Int J Chem React Eng 2010;8. https://doi.org/10.2202/1542-6580.2267/MACHINEREADABLECITATION/RIS.

[164] Farsi M, Jahanmiri A, Eslamloueyan R. Modeling and optimization of MeOH to DME in isothermal fixed-bed reactor. Int J Chem React Eng 2010;8. https://doi.org/10.2202/1542-6580.2063/MACHINEREADABLECITATION/RIS.

[165] Peláez R, Marín P, Díez FV, Ordóñez S. Direct synthesis of dimethyl ether in multi-tubular fixed-bed reactors: 2D multi-scale modelling and optimum design. Fuel Process Technol 2018;174:149–57. https://doi.org/10.1016/J.FUPROC.2018.02.025.

[166] Song D, Cho SY, Vu TT, Duong YHP, Kim E. Validation of a Fixed Bed Reactor Model for Dimethyl Ether Synthesis Using Pilot-Scale Plant Data. Catalysts 2021;11:1522. https://doi.org/10.3390/CATAL11121522.

[167] Lu WZ, Teng LH, Xiao WD. Simulation and experiment study of dimethyl ether synthesis from syngas in a fluidized-bed reactor. Chem Eng Sci 2004;59:5455–64. https://doi.org/10.1016/j.ces.2004.07.031.

[168] Abashar MEE. Dimethyl ether synthesis in a multi-stage fluidized bed reactor. Chem Eng Process Process Intensif 2017;122:172–80. https://doi.org/10.1016/J.CEP.2017.09.018.

[169] Koyunoğlu C, Karaca H, Soyhan HS. Modelling DME production from synthetic gases with a fluidized bed reactor: A CFD approach. Fuel 2021;304:121331. https://doi.org/10.1016/J.FUEL.2021.121331.

[170] Yousefi A, Eslamloueyan R, Kazerooni NM. Optimal conditions in direct dimethyl ether synthesis from syngas utilizing a dual-type fluidized bed reactor. Energy 2017;125:275–86. https://doi.org/10.1016/J.ENERGY.2017.02.085.

[171] Vakili R, Setoodeh P, Pourazadi E, Iranshahi D, Rahimpour MR. Utilizing differential evolution (DE) technique to optimize operating conditions of an integrated thermally coupled direct DME synthesis reactor. Chem Eng J 2011;168:321–32. https://doi.org/10.1016/J.CEJ.2011.01.032.

[172] Lei Z, Zou Z, Dai C, Li Q, Chen B. Synthesis of dimethyl ether (DME) by catalytic distillation. Chem Eng Sci 2011;66:3195–203. https://doi.org/10.1016/J.CES.2011.02.034.

[173] Bîldea CS, Győrgy R, Brunchi CC, Kiss AA. Optimal design of intensified processes for DME synthesis. Comput Chem Eng 2017;105:142–51. https://doi.org/10.1016/j.compchemeng.2017.01.004.

[174] Farsi M, Hallaji Sani A, Riasatian P. Modeling and operability of DME production from syngas in a dual membrane reactor. Chem Eng Res Des 2016;112:190–8. https://doi.org/10.1016/j.cherd.2016.06.019.

[175] Mardanpour MM, Sadeghi R, Ehsani MR, Nasr EM. Enhancement of dimethyl ether production with application of hydrogen-permselective Pd-based membrane in fluidized bed reactor. J Ind Eng Chem 2012;18:1157–65. https://doi.org/10.1016/J.JIEC.2012.01.012.

[176] Farniaei M, Abbasi M, Rasoolzadeh A, Rahimpour MR. Enhancement of methanol, DME and hydrogen production via employing hydrogen permselective membranes in a novel integrated thermally double-coupled two-membrane reactor. J Nat Gas Sci Eng 2013;14:158–73. https://doi.org/10.1016/j.jngse.2013.06.010.

[177] Bakhtyari A, Haghbakhsh R, Rahimpour MR. Investigation of thermally double coupled double membrane heat exchanger reactor to produce dimethyl ether and methyl formate. J Nat Gas Sci Eng 2016;32:185–97. https://doi.org/10.1016/J.JNGSE.2016.04.002.

[178] Yasari E. Improved dynamic performance of a thermally efficient reactor through water removal and defining new objective functions. Fuel Process Technol 2019;193:82–93. https://doi.org/10.1016/j.fuproc.2019.05.007.

[179] Bayat M, Asil AG. Efficient in-situ water adsorption for direct DME synthesis: Robust computational modeling and multi-objective optimization. J Nat Gas Sci Eng 2020;83:103587. https://doi.org/10.1016/J.JNGSE.2020.103587.

[180] Samimi F, Bayat M, Karimipourfard D, Rahimpour MR, Keshavarz P. A novel axial-flow spherical packed-bed membrane reactor for dimethyl ether synthesis: Simulation and optimization. J Nat Gas Sci Eng 2013;13:42–51. https://doi.org/10.1016/J.JNGSE.2013.03.001.

[181] Samimi F, Bayat M, Rahimpour MR, Keshavarz P. Mathematical modeling and optimization of DME synthesis in two spherical reactors connected in series. J Nat Gas Sci Eng 2014;17:33–41. https://doi.org/10.1016/J.JNGSE.2013.12.006.

[182] Farsi M, Asemani M, Rahimpour MR. Mathematical modeling and optimization of multi-stage spherical reactor configurations for large scale dimethyl ether production. Fuel Process Technol 2014;126:207–14. https://doi.org/10.1016/J.FUPROC.2014.04.029.

[183] Farsi M. DME production in multi-stage radial flow spherical membrane reactors: Reactor design and modeling. J Nat Gas Sci Eng 2014;20:366–72. https://doi.org/10.1016/J.JNGSE.2014.07.009.

[184] Hu J, Wang Y, Cao C, Elliott DC, Stevens DJ, White JF. Conversion of biomass syngas to DME using a microchannel reactor. Ind Eng Chem Res 2005;44:1722–7. https://doi.org/10.1021/IE0492707/ASSET/IMAGES/LARGE/IE0492707F00009.JPEG.

[185] Hayer F, Bakhtiary-Davijany H, Myrstad R, Holmen A, Pfeifer P, Venvik HJ. Synthesis of dimethyl ether from syngas in a microchannel reactor—Simulation and experimental study. Chem Eng J 2011;167:610–5. https://doi.org/10.1016/J.CEJ.2010.09.080.

[186] Hayer F, Bakhtiary-Davijany H, Myrstad R, Holmen A, Pfeifer P, Venvik HJ. Characteristics of integrated micro packed bed reactor-heat exchanger configurations in the direct synthesis of dimethyl ether. Chem Eng Process Process Intensif 2013;70:77–85. https://doi.org/10.1016/J.CEP.2013.03.021.

[187] Pérez-Miqueo I, Sanz O, Montes M. Highly Conductive Structured Catalytic Reactors for One-Step Synthesis of Dimethyl Ether. Ind Eng Chem Res 2021;60:6676–86. https://doi.org/10.1021/acs.iecr.0c05821.

[188] Ng KL, Chadwick D, Toseland BA. Kinetics and modelling of dimethyl ether synthesis from synthesis gas. Chem Eng Sci 1999;54:3587–92. https://doi.org/10.1016/S0009-2509(98)00514-4.

[189] Hadipour A, Sohrabi M. Synthesis of some bifunctional catalysts and determination of kinetic parameters for direct conversion of syngas to dimethyl ether. Chem Eng J 2008;137:294–301. https://doi.org/10.1016/j.cej.2007.04.039.

[190] Natta G. Synthesis of methanol. In: Emmett PH, editor. Catalysis, vol. 3. New York: Reinhold; 1955. p. 349–411.

[191] Leonov VE, Karavaev MM, Tsybina EN, Petrischeva GS. Kinetics of methanol synthesis on a low temperature catalyst. Kint Katal 1973;14:970–5.

[192] Klier K, Chatikavanij V, Herman RG, Simmons GW. Catalytic synthesis of methanol from COH_2: IV. The effects of carbon dioxide. J Catal 1982;74:343–60. https://doi.org/10.1016/0021-9517(82)90040-9.

[193] Chinchen GC, Hay CM, Vandervell HD, Waugh KC. The measurement of copper surface areas by reactive frontal chromatography. J Catal 1987;103:79–86. https://doi.org/10.1016/0021-9517(87)90094-7.

[194] Vanden BKM, Froment GF. A Steady-State Kinetic Model for Methanol Synthesis and the Water Gas Shift Reaction on a Commercial $Cu/ZnO/Al_2O_3$ Catalyst. J Catal 1996;161:1–10. https://doi.org/10.1006/jcat.1996.0156.

[195] Villa P, Forzatti P, Buzzi-Ferraris G, Garone G, Pasquon I. Synthesis of alcohols from carbon oxides and hydrogen. 1. Kinetics of the low-pressure methanol synthesis. Ind Eng Chem Process Des Dev 1985;24:12–9. https://doi.org/10.1021/i200028a003.

[196] Graaf GH, Scholtens H, Stamhuis EJ, Beenackers AACM. Intra-particle diffusion limitations in low-pressure methanol synthesis. Chem Eng Sci 1990;45:773–83. https://doi.org/10.1016/0009-2509(90)85001-T.

[197] Graaf GH, Stamhuis EJ, Beenackers AACM. Kinetics of low-pressure methanol synthesis. Chem Eng Sci 1988;43:3185–95. https://doi.org/10.1016/0009-2509(88)85127-3.

[198] Lim HW, Park MJ, Kang SH, Chae HJ, Bae JW, Jun KW. Modeling of the kinetics for methanol synthesis using $Cu/ZnO/Al_2O_3/ZrO_2$ catalyst: Influence of carbon dioxide during hydrogenation. Ind Eng Chem Res 2009;48:10448–55. https://doi.org/10.1021/ie901081f.

[199] Gates BC, Johanson LN. The dehydration of methanol and ethanol catalyzed by polystyrene sulfonate resins. J Catal 1969;14:69–76. https://doi.org/10.1016/0021-9517(69)90357-1.

[200] Kiviranta-Pääkkönen PK, Struckmann LK, Linnekoski JA, Krause OI. Dehydration of the Alcohol in the Etherification of Isoamylenes with Methanol and Ethanol. Ind Eng Chem Res 1998;37:18–24. https://doi.org/10.1021/IE970454D.

[201] Sierra I, Ereña J, Aguayo AT, Ateka A, Bilbao J. Kinetic modelling for the dehydration of methanol to dimethyl ether over γ-Al_2O_3. Chem Eng Trans 2013;32:613–8. https://doi.org/10.3303/cet1332103.

[202] Ha KS, Lee YJ, Bae JW, Kim YW, Woo MH, Kim HS, et al. New reaction pathways and kinetic parameter estimation for methanol dehydration over modified ZSM-5 catalysts. Appl Catal A Gen 2011;395:95–106. https://doi.org/10.1016/j.apcata.2011.01.025.

[203] Behloul CR, Commenge J-M, Castel C. Simulation of Reactors under Different Thermal Regimes and Study of the Internal Diffusional Limitation in a Fixed-Bed Reactor for the Direct Synthesis of Dimethyl Ether from a CO_2-Rich Input Mixture and H_2. Ind Eng Chem Res 2021;60:1602–23. https://doi.org/10.1021/acs.iecr.0c05535.

[204] Aguayo AT, Ereña J, Mier D, Arandes JM, Olazar M, Bilbao J. Kinetic modeling of dimethyl ether synthesis in a single step on a $CuO-ZnO-Al_2O_3/\gamma-Al_2O_3$ catalyst. Ind Eng Chem Res 2007;46:5522–30. https://doi.org/10.1021/ie070269s.

[205] Shim HM, Lee SJ, Yoo YD, Yun YS, Kim HT. Simulation of DME synthesis from coal syngas by kinetics model. Korean J Chem Eng 2009;26:641–8. https://doi.org/10.1007/S11814-009-0107-9.

[206] Sierra I, Ereña J, Aguayo AT, Olazar M, Bilbao J. Deactivation kinetics for direct dimethyl ether synthesis on a $CuO-ZnO-Al_2O_3/\gamma-Al_2O_3$ Catalyst. Ind Eng Chem Res 2010;49:481–9. https://doi.org/10.1021/ie900978a.

[207] Ateka A, Rodriguez-Vega P, Cordero-Lanzac T, Bilbao J, Aguayo AT. Model validation of a packed bed LTA membrane reactor for the direct synthesis of DME from CO/CO_2. Chem Eng J 2021;408:127356. https://doi.org/10.1016/j.cej.2020.127356.

[208] Berčič G, Levec J. Catalytic Dehydration of Methanol to Dimethyl Ether. Kinetic Investigation and Reactor Simulation. Ind Eng Chem Res 1993;32:2478–84. https://doi.org/10.1021/ie00023a006.

[209] Nie Z, Liu H, Liu D, Ying W, Fang D. Intrinsic Kinetics of Dimethyl Ether Synthesis from Syngas. J Nat Gas Chem 2005;14:22–8.

[210] An X, Zuo YZ, Zhang Q, Wang DZ, Wang JF. Dimethyl ether synthesis from CO_2 hydrogenation on a $CuO-ZnO-Al_2O_3-ZrO_2$/HZSM-5 bifunctional catalyst. Ind Eng Chem Res 2008;47:6547–54. https://doi.org/10.1021/ie800777t.

[211] Tao KY. Reaction kinetic study of methanol dehydration to dimethyl ether. J Fuel Chem Technol 1993;4:387.

[212] Park N, Park MJ, Lee YJ, Ha KS, Jun KW. Kinetic modeling of methanol synthesis over commercial catalysts based on three-site adsorption. Fuel Process Technol 2014;125:139–47. https://doi.org/10.1016/J.FUPROC.2014.03.041.

[213] Peláez R, Bryce E, Marín P, Ordóñez S. Catalyst deactivation in the direct synthesis of dimethyl ether from syngas over $CuO/ZnO/Al_2O_3$ and γ-Al_2O_3 mechanical mixtures. Fuel Process Technol 2018;179:378–86. https://doi.org/10.1016/J.FUPROC.2018.07.029.

[214] Silva VMTM, Pereira CSM, Rodrigues AE. PermSMBR-A new hybrid technology: Application on green solvent and biofuel production. AIChE J 2011;57:1840–51. https://doi.org/10.1002/aic.12381.

[215] Abashar MEE, Al-Rabiah AA. Investigation of the efficiency of sorption-enhanced methanol synthesis process in circulating fast fluidized bed reactors. Fuel Process Technol 2018;179:387–98. https://doi.org/10.1016/j.fuproc.2018.07.028.

[216] Iliuta I, Iliuta MC, Larachi F. Sorption-enhanced dimethyl ether synthesis-Multiscale reactor modeling. Chem Eng Sci 2011;66:2241–51. https://doi.org/10.1016/j.ces.2011.02.047.

[217] Van Kampen J, Boon J, Vente J, Van Sint AM. Sorption enhanced dimethyl ether synthesis under industrially relevant conditions: Experimental validation of pressure swing regeneration. React Chem Eng 2021;6:244–57. https://doi.org/10.1039/d0re00431f.

[218] van Kampen J, Boon J, Vente J, van Sint Annaland M. Van Sint Annaland M. Sorption enhanced dimethyl ether synthesis for high efficiency carbon conversion: Modelling and cycle design. J CO2 Util 2020;37:295–308.

[219] Guffanti S, Visconti CG, van Kampen J, Boon J, Groppi G. Reactor modelling and design for sorption enhanced dimethyl ether synthesis. Chem Eng J 2021;404:126573. https://doi.org/10.1016/J.CEJ.2020.126573.

[220] Guffanti S, Visconti CG, Groppi G. Model Analysis of the Role of Kinetics, Adsorption Capacity, and Heat and Mass Transfer Effects in Sorption Enhanced Dimethyl Ether Synthesis. Ind Eng Chem Res 2021;60:6767–83. https://doi.org/10.1021/acs.iecr.1c00521.

[221] Dieterich V, Buttler A, Hanel A, Spliethoff H, Fendt S. Power-to-liquid via synthesis of methanol, DME or Fischer–Tropsch-fuels: a review. Energy Environ Sci 2020;13:3207–52. https://doi.org/10.1039/D0EE01187H.

[222] Hamedi H, Brinkmann T. Valorization of CO_2 to DME using a membrane reactor: A theoretical comparative assessment from the equipment to flowsheet level. Chem Eng J Adv 2022;10:100249. https://doi.org/10.1016/J.CEJA.2022.100249.

[223] Farsi M, Jahanmiri A. Dynamic modeling and operability analysis of a dual-membrane fixed bed reactor to produce methanol considering catalyst deactivation. J Ind Eng Chem 2014;20:2927–33. https://doi.org/10.1016/J.JIEC.2013.11.030.

[224] Gogate MR. The direct dimethyl ether (DME) synthesis process from syngas I. Process feasibility and chemical synergy in one-step LPDMEtm process. Pet. Sci Technol 2018;36:547–54. https://doi.org/10.1080/10916466.2018.1428628.

[225] Mokhtari M, Chaouki J. Effect of solid loading and particle size on the phase holdup distribution and bubble behaviour in a pilot-scale slurry bubble column. Chem Eng Sci 2021;243:116732. https://doi.org/10.1016/J.CES.2021.116732.

[226] Li W, Zhou G, Sun J, Guo Y, Wang R. Impacts of Particle Properties on Gas Holdup under Four Flow Regimes in Three-Phase Bubble Columns. Chem Eng Technol 2021;44:2347–54. https://doi.org/10.1002/ceat.202100291.

[227] Shirzad M, Karimi M, Silva JAC, Rodrigues AE. Moving Bed Reactors: Challenges and Progress of Experimental and Theoretical Studies in a Century of Research. Ind Eng Chem Res 2019;58:9179–98. https://doi.org/10.1021/acs.iecr.9b01136.

[228] Cordero-Lanzac T, Aguayo AT, Bilbao J. Reactor-Regenerator System for the Dimethyl Ether-to-Olefins Process over HZSM-5 Catalysts: Conceptual Development and Analysis of the Process Variables. Ind Eng Chem Res 2020;59:14689–702. https://doi.org/10.1021/acs.iecr.0c02276.

[229] Hafeez S, Harkou E, Al-Salem SM, Goula MA, Dimitratos N, Charisiou ND, et al. Hydrogenation of carbon dioxide (CO_2) to fuels in microreactors: a review of set-ups and value-added chemicals production. React Chem Eng 2022;7(4):795–812.

[230] Koybasi HH, Hatipoglu C, Avci AK. Sustainable DME synthesis from CO_2–rich syngas in a membrane assisted reactor–microchannel heat exchanger system. J CO2 Util 2021;52:101660.

[231] Koybasi HH, Avci AK. Modeling of a membrane integrated catalytic microreactor for efficient DME production from syngas with CO_2. Catal Today 2022;383:133–45. https://doi.org/10.1016/j.cattod.2020.10.020.

[232] Diban N, Urtiaga AM, Ortiz I, Ereña J, Bilbao J, Aguayo AT. Influence of the membrane properties on the catalytic production of dimethyl ether with in situ water removal for the successful capture of CO_2. Chem Eng J 2013;234:140–8. https://doi.org/10.1016/j.cej.2013.08.062.

[233] Rahimpour MR, Dehghani Z. Membrane reactors for methanol synthesis from forest-derived feedstocks. Membr Technol Biorefining 2016:383–410. https://doi.org/10.1016/B978-0-08-100451-7.00015-3.

[234] Farsi M, Jahanmiri A. Dynamic modeling of a H_2O-permselective membrane reactor to enhance methanol synthesis from syngas considering catalyst deactivation. J Nat Gas Chem 2012;21:407–14. https://doi.org/10.1016/S1003-9953(11)60383-6.

[235] Bayat M, Dehghani Z, Rahimpour MR. Membrane/sorption-enhanced methanol synthesis process: Dynamic simulation and optimization. J Ind Eng Chem 2014;20:3256–69. https://doi.org/10.1016/j.jiec.2013.12.007.

[236] Struis RPW, Stucki S. Verification of the membrane reactor concept for the methanol synthesis. Appl Catal A Gen 2001;216:117–29. https://doi.org/10.1016/S0926-860X(01)00548-8.

[237] Lee SB, Cho W, Park DK, Yoon ES. Simulation of fixed bed reactor for dimethyl ether synthesis. Korean J Chem Eng 2006;23:522–30. https://doi.org/10.1007/BF02706789.

[238] Sea B, Lee KH. Synthesis of dimethyl ether from methanol using alumina-silica membrane reactor. Desalination 2006;200:689–91. https://doi.org/10.1016/j.desal.2006.03.467.

[239] Espinoza RL, Du Toit E, Santamaria J, Menendez M, Coronas J, Irusta S. Use of membranes in fischer-tropsch reactors. Stud Surf Sci Catal 2000;130:389–94. https://doi.org/10.1016/S0167-2991(00)80988-X.

[240] Espinoza. Production of hydrocarbons. US 6,403,660 B1, 2000.

[241] Rohde MP, Schaub G, Khajavi S, Jansen JC, Kapteijn F. Fischer-Tropsch synthesis with in situ H_2O removal - Directions of membrane development. Microporous Mesoporous Mater 2008;115:123–36. https://doi.org/10.1016/j.micromeso.2007.10.052.

[242] Fedosov DA, Smirnov AV, Shkirskiy VV, Voskoboynikov T, Ivanova II. Methanol dehydration in NaA zeolite membrane reactor. J Memb Sci 2015;486:189–94. https://doi.org/10.1016/j.memsci.2015.03.047.

[243] Rohde MP, Unruh D, Schaub G. Membrane application in Fischer-Tropsch synthesis to enhance CO_2 hydrogenation. Ind Eng Chem Res 2005;44:9653–8. https://doi.org/10.1021/ie050289z.

[244] Reddy GK, Smirniotis PG. Mechanism and kinetics of the WGS reaction. Water Gas Shift React. Res Dev Appl, Elsevier Inc 2015:225–61.

[245] Gallucci F, Paturzo L, Basile A. An experimental study of CO_2 hydrogenation into methanol involving a zeolite membrane reactor. Chem Eng Process Process Intensif 2004;43:1029–36. https://doi.org/10.1016/j.cep.2003.10.005.

[246] Lee J, Park HG, Hyeon MH, Kim BG, Kim SK, Moon SY. Low-temperature CO_2 hydrogenation overcoming equilibrium limitations with polyimide hollow fiber membrane reactor. Chem Eng J 2021;403:126457–66. https://doi.org/10.1016/j.cej.2020.126457.
[247] Gorbe J, Lasobras J, Francés E, Herguido J, Menéndez M, Kumakiri I, et al. Preliminary study on the feasibility of using a zeolite A membrane in a membrane reactor for methanol production. Sep Purif Technol 2018;200:164–8. https://doi.org/10.1016/j.seppur.2018.02.036.
[248] Iliuta I, Larachi F, Fongarland P. Dimethyl ether synthesis with in situ H_2O removal in fixed-bed membrane reactor: Model and simulations. Ind Eng Chem Res 2010;49:6870–7. https://doi.org/10.1021/ie901726u.
[249] Diban N, Urtiaga AM, Ortiz I, Ereña J, Bilbao J, Aguayo AT. Improved performance of a pbm reactor for simultaneous CO_2 capture and DME synthesis. Ind Eng Chem Res 2014;53:19479–87. https://doi.org/10.1021/ie503663h.
[250] Poto S, Gallucci F, Neira d'Angelo MF. Direct conversion of CO_2 to dimethyl ether in a fixed bed membrane reactor: Influence of membrane properties and process conditions. Fuel 2021;302:121080. https://doi.org/10.1016/j.fuel.2021.121080.
[251] De Falco M, Capocelli M, Basile A. Selective membrane application for the industrial one-step DME production process fed by CO_2 rich streams: Modeling and simulation. Int J Hydrogen Energy 2017;42:6771–86. https://doi.org/10.1016/j.ijhydene.2017.02.047.
[252] De Falco M, Capocelli M, Giannattasio A. Membrane Reactor for one-step DME synthesis process: Industrial plant simulation and optimization. J CO2 Util 2017;22:33–43. https://doi.org/10.1016/j.jcou.2017.09.008.
[253] Ateka A, Ereña J, Bilbao J, Aguayo AT. Strategies for the Intensification of CO_2 Valorization in the One-Step Dimethyl Ether Synthesis Process. Ind Eng Chem Res 2020;59:713–22. https://doi.org/10.1021/acs.iecr.9b05749.
[254] Koybasi HH, Hatipoglu C, Avci AK. Comparison of intensified reactor systems for one–step conversion of CO_2–containing syngas to DME. Chem Eng Process - Process Intensif 2021;167:108538. https://doi.org/10.1016/J.CEP.2021.108538.
[255] Ji G, Wang G, Hooman K, Bhatia S, Diniz da Costa JC. Computational fluid dynamics applied to high temperature hydrogen separation membranes. Front Chem Sci Eng 2012.3–12.;2012(61):6. https://doi.org/10.1007/S11705-011-1161-5.
[256] van Kampen J, Boon J, van Berkel F, Vente J, van Sint AM. Steam separation enhanced reactions: Review and outlook. Chem Eng J 2019;374:1286–303. https://doi.org/10.1016/J.CEJ.2019.06.031.
[257] Wang N, Liu Y, Huang A, Caro J. Hydrophilic SOD and LTA membranes for membrane-supported methanol, dimethylether and dimethylcarbonate synthesis Microporous Mesoporous. Mater 2015;207:33–8. https://doi.org/10.1016/j.micromeso.2014.12.028.
[258] Vakili R, Pourazadi E, Setoodeh P, Eslamloueyan R, Rahimpour MR. Direct dimethyl ether (DME) synthesis through a thermally coupled heat exchanger reactor. Appl Energy 2011;88:1211–23. https://doi.org/10.1016/j.apenergy.2010.10.023.
[259] Hu Y, Nie Z, Fang D. Simulation and model design of pipe-shell reactor for the direct synthesis of dimethyl ether from syngas. J Nat Gas Chem 2008;17:195–200. https://doi.org/10.1016/S1003-9953(08)60051-1.
[260] Rodriguez-Vega P, Ateka A, Kumakiri I, Vicente H, Ereña J, Aguayo AT, et al. Experimental implementation of a catalytic membrane reactor for the direct synthesis of DME from H_2+CO/CO_2. Chem Eng Sci 2021;234:116396. https://doi.org/10.1016/J.CES.2020.116396.
[261] Cordero-Lanzac T, Aguayo AT, Gayubo AG, Castaño P, Bilbao J. Simultaneous modeling of the kinetics for n-pentane cracking and the deactivation of a HZSM-5 based catalyst. Chem Eng J 2018;331:818–30. https://doi.org/10.1016/j.cej.2017.08.106.
[262] Ateka A, Ereña J, Sánchez-Contador M, Perez-Uriarte P, Bilbao J, Aguayo AT. Capability of the direct dimethyl ether synthesis process for the conversion of carbon dioxide. Appl Sci 2018;8:677–90. https://doi.org/10.3390/app8050677.
[263] Ozturk NF, Avci AK. Intensified dimethyl ether production from synthesis gas with CO_2. Chem Eng J 2019;370:885–96. https://doi.org/10.1016/J.CEJ.2019.03.210.
[264] Tozar U, Avci AK. Strategies for improving CO_2 utilization in microchannel enabled production of dimethyl ether. Chem Eng Process - Process Intensif 2020;151:107914. https://doi.org/10.1016/J.CEP.2020.107914.
[265] Yue M, Lambert H, Pahon E, Roche R, Jemei S, Hissel D. Hydrogen energy systems: A critical review of technologies, applications, trends and challenges. Renew Sustain Energy Rev 2021;146:111180. https://doi.org/10.1016/J.RSER.2021.111180.
[266] Maestre VM, Ortiz A, Ortiz I. Challenges and prospects of renewable hydrogen-based strategies for full decarbonization of stationary power applications. Renew Sustain Energy Rev 2021;152:111628. https://doi.org/10.1016/J.RSER.2021.111628.
[267] Yang F, Wang T, Deng X, Dang J, Huang Z, Hu S, et al. Review on hydrogen safety issues: Incident statistics, hydrogen diffusion, and detonation process. Int J Hydrogen Energy 2021;46:31467–88. https://doi.org/10.1016/J.IJHYDENE.2021.07.005.
[268] Farsi M, Fekri Lari M, Rahimpour MR. Development of a green process for DME production based on the methane tri-reforming. J Taiwan Inst Chem Eng 2020;106:9–19. https://doi.org/10.1016/J.JTICE.2019.10.001.
[269] Arregi A, Amutio M, Lopez G, Bilbao J, Olazar M. Evaluation of thermochemical routes for hydrogen production from biomass: A review. Energy Convers Manag 2018;165:696–719. https://doi.org/10.1016/J.ENCONMAN.2018.03.089.
[270] Zhang T-Q, Malik FR, Jung S, Kim Y-B. Hydrogen production and temperature control for DME autothermal reforming process. Energy 2022;239:121980.